Inorganic Chemistry

pubs.acs.org/IC

Article

Ab Initio Thermochemistry of the First-Row Transition Metal Tris(Acetylacetonates): Refined, Revisited, and Recommended

Andrey D. Moshchenkov, Alexander S. Ryzhako, Arseniy A. Otlyotov, and Yury Minenkov*

Cite This: *Inorg. Chem.* 2025, 64, 21405−21418

Read Online

ACCESS | Metrics & More | Article Recommendations | Supporting Information

ABSTRACT: Gas-phase enthalpies of formation ($\Delta_fH°$(g, 298 K)) of Sc, Ti, V, Cr, Mn, Fe, and Co tris(acetylacetonates) were predicted using the reaction-based approach implemented in the recently developed program. Energies of working reactions were computed by employing the Feller−Peterson−Dixon composite scheme in conjunction with the DLPNO−CCSD(T)/CBS and also using several DFT model chemistries. A careful analysis of the literature data on the experimental and theoretical $\Delta_fH°$ (g, 298 K) of the relevant transition metal oxides, fluorides, and chlorides revealed the most reliable values to be used as references in the reaction-based approach. The predicted enthalpies of formation of $M(acac)_3$ complexes were utilized for the rationalization of the literature-available experimental data. The difference between theoretical and experimental $\Delta_fH°$ (g, 298 K) falls within the error margins in the case of $V(acac)_3$, $Fe(acac)_3$, and $Co(acac)_3$. For $Mn(acac)_3$, the theoretical $\Delta_fH°$ (g, 298 K) agrees better with the value obtained from an older study. In the case of $Sc(acac)_3$ and $Cr(acac)_3$, the discrepancies between experiment and theory reach 13.1 and 6.1 kcal mol^{-1}, respectively. For $Ti(acac)_3$, the predicted $\Delta_fH°$ (g,298 K) = −374.8 ± 4.5 kcal mol^{-1} is probably the only currently available value.

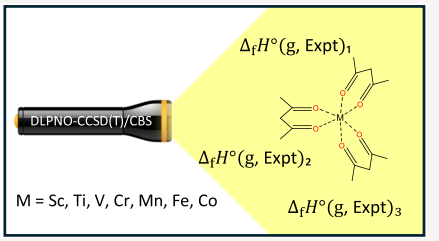

1. INTRODUCTION

For the past three decades, transition metal tris(acetylacetonates) have established themselves as prospective catalysts or catalytic supports,[1−4] films stabilizers,[5] and precursors for metal−organic chemical vapor deposition (MOCVD).[6−9] In particular, Sc(III) tris(acetylacetonate) and its derivatives were shown to be prospective MOCVD precursors for oxide film deposition.[6,7] Other metal complexes can be used as effective catalysts in transesterification ($Fe(acac)_3$)[10] and cross-coupling reactions ($Co(acac)_3$, $Mn(acac)_3$)[11,12] and Ziegler−Natta polymerization ($V(acac)_3$, $Mn(acac)_3$).[13,14] Additionally, Cr(III) and V(III) tris(acetylacetonates) are exploited as components in high-capacity redox flow batteries.[15,16]

The high importance of these compounds has stimulated a number of studies focused on the determination of their fundamental thermodynamic characteristics. However, as it was recently shown for $Fe(acac)_3$, the results of independent experimental measurements can be widely scattered, with the difference between the solid-state enthalpies of formation reaching 40.6 kcal mol^{-1}.[17] A similar problem in the case of other metal β-diketonates was mentioned by Zherikova and co-workers.[18]

In the last several decades, computational chemistry has emerged as a powerful tool to verify experimental thermochemical data.[19,20] It should, however, be mentioned that the computational cost of high-level ab initio approaches rises dramatically with the molecular size, making them prohibitively expensive even for medium-sized species. Several steps can be taken to reduce computational demands. First, instead of the "gold standard" canonical coupled-cluster CCSD(T) method,[21] one can use its localized version, such as the DLPNO−CCSD(T) approach of Neese and co-workers.[22−28] Second, following the flexible Feller−Peterson−Dixon (FPD) scheme,[29−31] the total energy of a system can be split into separate parts evaluated independently using computationally efficient yet still accurate theoretical approximations.

Electronic energies from quantum chemical calculations can be used to derive gas-phase enthalpies of formation via the reaction-based approach combining a target molecule (with an unknown $\Delta_fH°$ (g)) and reference molecules, for which their accurate $\Delta_fH°$ (g) values are available in the literature or databases. The key advantage of this approach lies in the pronounced error cancellation in the theoretical $\Delta_rH°$ compared to atomization reactions.[19] In our group, this method has been recently implemented in the reaction generator (RG) program[32,33] and extensively tested on various classes of compounds.[17,34−37] With regard to Fe(III) tris(β-diketonates), it helped to validate scattered experimental solid-state enthalpies of formation and define a consistent data set of $\Delta_fH°$ (g) values in gaseous and crystalline states.[17]

Received: July 4, 2025
Revised: October 7, 2025
Accepted: October 8, 2025
Published: October 20, 2025

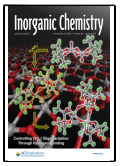

In the present contribution, we critically evaluate the reliability of the literature-available experimental enthalpies of formation of the first-row transition metal (Sc, V, Cr, Mn, Fe, Co) tris(acetylacetonates) and predict the gas-phase enthalpy of formation of $Ti(acac)_3$. The performance of the computationally efficient DFT approximations as cheaper substitutes of the sophisticated DLPNO−CCSD(T)/CBS-based FPD protocol is examined. In addition, a database of $\Delta_f H°$ (g, 298 K) of the small reference transition metal compounds has been compiled based on the thorough comparison of experimental and theoretical values.

2. COMPUTATIONAL DETAILS

2.1. Reference ATcT Enthalpies of Formation. The reaction-based Feller−Peterson−Dixon approach requires a set of compounds with known enthalpies of formation to be used as references in the working reactions. It is essential to identify reliable thermochemical data to minimize the impact of experimental error on the predicted enthalpy of the formation of the target compound. The active thermochemical tables (ATcT) developed in the Argonne National Laboratory[38−41] were used as a source of reliable data for enthalpies of formation of organic compounds (see Table S1). Small reference transition metal containing compounds were carefully selected as described in Section 3.1.

2.2. Quantum Chemical Calculations. *2.2.1. Geometry Optimization and Frequencies.* The optimized spatial structures of $M(acac)_3$ complexes and all reference species were obtained with the use of hybrid functional PBE0[42] and triple-ζ valence-polarized def2-TZVP[43] basis set of the Karlsruhe group as implemented in the ORCA 6 software package.[44] Tighter-than-default optimization settings, such as large DEFGRID3 integration grid and convergence tolerances *TolE* = 1×10^{-6} a.u., *TolRMSG* = 3×10^{-5} a.u., *TolMaxG* = 1×10^{-4} a.u. were employed. The atom-pairwise dispersion correction with the Becke−Johnson damping scheme (D3BJ) was included.[45,46] The resolution of the identity (RI) treatment of the Coulomb term and seminumerical integration of the exchange term (COSX)[47,48] were utilized to accelerate the calculations with appropriate def2/J auxiliary basis sets.[49]

Harmonic frequencies were obtained for all optimized geometries, scaled by a factor of 0.983 derived[50] for the PBE0-D3/TZVP method, and used for the computation of thermal corrections to enthalpies (H_{CORR}) via the modified ideal gas, rigid rotor, and harmonic oscillator (msRRHO(τ = 100 cm^{-1})) approach of Grimme,[51,52] recently extended for enthalpies.[53]

Spin-state splittings were calculated for Ti, V, and Mn complexes and are listed in Table S2. Based on the previous studies, multiplicities 4, 5, and 6 were assigned to $Cr(acac)_3$,[54] $Mn(acac)_3$,[55,56] and $Fe(acac)_3$,[57] respectively. $Sc(acac)_3$[58] and $Co(acac)_3$[54] were treated as singlets. In addition, all considered $M(acac)_3$ complexes are well-established[54,56,59,60] to exist in the form of a single conformer, and no additional conformer search was performed.

2.2.2. Single-Point Energy Evaluation. The proposed reaction-based Feller−Peterson−Dixon approach was adopted from our recent study[35]

$$\Delta_r H° = \Delta E_{CBS} + \Delta E_{CV} + \Delta E_{PNO} + \Delta E_{IT} + \Delta E_{SR} + \Delta H_{CORR} \quad (1)$$

where ΔE_{CBS} is a complete basis set extrapolated DLPNO−CCSD(T)[22−28] reaction energy change; ΔE_{CV} refers to the core−valence electron correlation correction; ΔE_{PNO} stands for the correction stemming from the complete PNO space extrapolation; ΔE_{IT} is an effect of iterative triples inclusion; ΔE_{SR} is the scalar relativistic (SR) effect; and ΔH_{CORR} is a thermal correction to convert reaction energies into the corresponding enthalpies.

Total reaction energies ΔE_{CBS} were calculated with the use of the correlation-consistent basis sets cc-pV*n*Z (n = T, Q) on nonmetal atoms (H, C, O, Cl, F)[61,62] and cc-pwCV*n*Z-PP with weighted-core functions on the transition metal atoms,[63] which will be henceforth referred to as cc-p(wC)V*n*Z(-PP) basis sets. Valence and subvalence ($3s^2 3p^6 4s^2 3d^x$) electrons on the metal atoms were correlated in all of the DLPNO−CCSD(T) calculations in this work. Core electrons ($1s^2 2s^2 2p^6$) were replaced with the Stuttgart−Dresden effective core potentials (ECPs).[64]

Basis set incompleteness error (BSIE) was treated by the recommended[65,66] Martin[67] complete basis set extrapolation scheme for n = T and Q

$$E^n_{\text{DLPNO-CCSD(T)}} = E^{\infty}_{\text{DLPNO-CCSD(T)}} + \frac{1}{\left(n + \frac{1}{2}\right)^4} \quad (2)$$

Auxiliary correlation fitting basis sets cc-pV*n*Z/C of Weigend et al.[68] were also employed as required in the RI approximation. Due to the absence of cc-pwCV*n*Z/C basis sets for 3d-transition metal atoms, they were generated by the "AutoAUX" routine.[69]

The effect of the core−valence electron correlation ΔE_{CV} was estimated at the DLPNO−CCSD(T)/cc-pwCV*n*Z(-PP) (n = D and T) level and *TightPNO* settings via the difference between "all-electron" (AE) and "frozen-core" (FC) approaches. In the AE approximation, the electrons belonging to the subvalence shells ($1s^2$ for C, O, F atoms and $2s^2 2p^6$ for Cl) were included in the correlation procedure by modifying *N_Core* values. On the other hand, FC implies the same (default) *N_Core* settings as for the ΔE_{CBS} part. For metal atoms, their $3s^2 3p^6 4s^2 3d^x$ electrons were correlated in both FC and AE calculations. Then, the energy difference ΔE_{CV} was extrapolated to the scheme described above.

The PNO space truncation error was addressed by introducing the ΔE_{PNO} correction. It was calculated as the difference between the complete PNO space (CPS)[70] extrapolated and *NormalPNO* energies. Considering E^X and E^Y as the energies with different T_{CutPNO} = 10^{-6} and 10^{-7} settings within the DLPNO−CCSD(T)/cc-p(wC)VTZ(-PP)/*TightPNO* method, the CPS(6/7) extrapolation scheme is performed according to the equation:

$$E^{CPS} = E^X + 1.5(E^Y - E^X) \quad (3)$$

The effect of iterative triples (T_1)[71,72] inclusion instead of their semicanonical (T) counterparts, ΔE_{IT}, was derived from the difference between DLPNO−CCSD(T_1) and DLPNO−CCSD(T) single-point energies with cc-p(wC)VTZ(-PP) basis sets.

Correction for the scalar relativistic effects, ΔE_{SR}, was computed as the difference between FC DLPNO−CCSD(T) reaction energies obtained with the standard second-order Douglas−Kroll−Hess Hamiltonian (DKH2) and the corresponding cc-p(wC)VTZ-DK[73−76] basis sets and their FC DLPNO−CCSD(T)/cc-p(wC)VTZ(-PP) counterparts.

https://doi.org/10.1021/acs.inorgchem.5c03069
Inorg. Chem. 2025, 64, 21405−21418

Table 1. Gas-Phase Enthalpies of Formation of Selected First-Row Transition Metal Compounds at 298 K[a]

reference species	experimental $\Delta_f H°$ (g, 298 K)[b]	theoretical $\Delta_f H°$ (g, 298 K)[b,c,d]
ScF_3	**−302.9 ± 3.2**;[100] −299.7 ± 3.6;[101] −300.4 ± 3.6;[102] −300.2 ± 1.9;[103] −297.8 ± 3.6;[104] −290.5 ± 1.4[105]	−302.5 ± 0.4[106] [DLPNO−CCSD(T1)]; −302.3,[107e] [CCSD(T)/CBS]; *−297.1*[108] [MP2/CBS] (avg: **−302.4**)
$ScCl_3$	**−160.5 ± 2.1**;[100] −166.1 ± 2.9[104]	**−162.8 ± 0.8**[106] [DLPNO−CCSD(T1)]; −164.9[108] [MP2/CBS]; *−163.9*[109] [G4(MP2)]
ScF	−31.2 ± 0.8;[105] **−33.9 ± 3.4**;[102] −34.0 ± 4.1[100]	−32.4,[107e] [CCSD(T)/CBS]; −34.2,[110e] [CCSD(T)/CBS]; *−33.2*[108] [MP2/CBS] (avg: **−33.3**)
TiO	**13.7 ± 2.2**;[100] 13 ± 2.2[111]	**13.9**[112] [CCSDTQ/CBS]; *16.2*[108] [MP2/CBS]; *16.0*[109] [G4(MP2)]
TiO_2	**−71.0 ± 5.1**;[100] −73 ± 3[111]	−67.9[113] [CCSD(T)-DK/CBS]; −71.7[112] [CCSDTQ/CBS]; −67.8[114] [CCSD(T)/CBS]; −69.6[115] [CCSD(T)/CBS]; −70.5[115] [CCSD(T)/PW91/CBS]; −69.4[115] [BCCD(T)/CBS]; −68.2[116] [CCSD(T)/CBS]; −67.9[117] [DLPNO−CCSD(T)/CBS]; *−67.7*[108] [MP2/CBS] (avg: **−69.3**)
TiF_4	**−370.8 ± 0.5**[100,111]	−374.2[118] [CCSD(T)/CBS]; −373.4[117] [DLPNO−CCSD(T)/CBS]; *−373.9*[108] [MP2/CBS]; *−369.5*[109] [G4(MP2)] (avg: **−373.8**)
$TiCl_4$	**−182.4 ± 0.7**[100,111,119−121]	−181.5[114] [CCSD(T)/CBS]; −181.9[118] [CCSD(T)/CBS]; *−184.4*[108] [MP2/CBS] (avg: **−181.7**)
$TiOCl_2$	−130.4;[111] −137.9[122]	−143.2[117] [DLPNO−CCSD(T)/CBS]; −141.8[114] [CCSD(T)/CBS]; −142.9[123] [CCSD(T)/CBS]; −143.5[124] [CCSD(T)/CBS]; *−143.2*[108] [MP2/CBS] (avg: **−142.9**)[f]
VO	**31.8 ± 2.0**;[125] 36.2 ± 10;[100] 30.5 ± 5[111]	32.0[98] [CCSD(T)-DK/CBS]; 31.8[126] [CCSD(T)/CBS]; 29.0[126] [CCSD(T)/PW91/CBS]; 31.3[127] [CCSD(T)-F12b/CBS]; 32.3[128] [CCSD(T)/CBS]; *35.0*[109] [G4(MP2)]; *32.8*[108] [MP2/CBS] (avg: **31.3**)
VO_2	**−41.6 ± 3.3**;[125] −55.6[111]	−39.1[98] [CCSD(T)-DK/CBS]; −42.2[127] [CCSD(T)-F12b/CBS]; −38.4[128] [CCSD(T)/CBS]; *−39.8*[108] [MP2/CBS] (avg: **−39.9**)
CrO	**45.0 ± 10.0**;[111] 43.6 ± 1.6[129]	46.0,[130e] [CCSD(T)/CBS]; 47.7[126] [CCSD(T)/CBS]; 45.9[126] [CCSD(T)/PW91/CBS]; 47.4[131] [CCSD(T)/CBS]; *44.3*[108] [MP2/CBS] (avg: **46.8**)
CrO_3	−77.3 ± 1.0;[129] −70.5 ± 20;[100] −70.4 ± 10[111]	−67.7[115] [CCSD(T)/PW91/CBS]; −66.5[115] [BCCD(T)/CBS]; −61.6[115] [CCSD(T)/CBS]; −64.3[98] [CCSD(T)-DK/CBS]; −62.3[132] [CCSD(T)-DK/CBS]; −68.5[131] [CCSD(T)/CBS]; −67.6[127] [CCSD(T)-F12b/CBS]; −63.3[127] [CCSD(T)/CBS]; *−69.3*[108] [MP2/CBS]; *−81.6*[109] [G4(MP2)] (avg: **−65.2**)[f]
CrCl	**33.7 ± 1.6**;[133] 31.0 ± 0.6;[129] 36.4;[100] 33.1;[134d]	33.1[126] [CCSD(T)/PW91/CBS]; 35.8[126] [CCSD(T)/CBS]; 32.4[135] [CCSD(T)]; *35.0*[109] [G4(MP2)]; *34.6*[108] [MP2/CBS] (avg: **33.8**)
$MnCl_2$	**−62.6 ± 1.0**;[133] −63.0 ± 0.5[100]	**−60.3**[128] [CBS-CCSD(T)]; *−60.3*[108] [MP2/CBS]
MnCl	**15.6 ± 1.8**;[133] 11.3;[100] 15.8[133]	15.0[126] [CCSD(T)/CBS]; 14.8[126] [CCSD(T)/PW91/CBS]; 14.5[127] [CCSD(T)-F12b/CBS]; 16.5[135] [CCSD(T)]; *12.8*[109] [G4(MP2)]; *16.0*[108] [MP2/CBS] (avg: **15.2**)
MnF	**−19.9 ± 3.0**;[100] −14.5 ± 4.0;[136] −20.0 ± 5.0;[137] −20.3 ± 3.0[138]	**−18.0**[135] [CCSD(T)]; *−19.4*[108] [MP2/CBS]
FeCl	**45.0 ± 3.0**,[100f]; 49.5 ± 1.6;[133] 60.0[111]	47.5[135] [CCSD(T)]; 46.5[126] [CCSD(T)/CBS]; 46.3[126] [CCSD(T)/PW91/CBS]; 47.2[127] [CCSD(T)-F12b/CBS]; *46.0*[109] [G4(MP2)]; *45.3*[139] [est-QCISD(T)/WHext]; *47.8*[108] [MP2/CBS] (avg: **46.9**)
$FeCl_2$	**−32.8 ± 1.0**;[133] −31.7 ± 0.2;[100] −33.7 ± 0.5[111]	−34.8[135] [CCSD(T)]; −33.1[127] [CCSD(T)-F12b/CBS]; −32.1[128] [CCSD(T)/CBS]; −32.5[98] [CCSD(T)-DK/CBS]; *−35.8*[139] [est-QCISD(T)/WHext]; *−29.6*[109] [G4(MP2)]; *−32.5*[108] [MP2/CBS] (avg: **−33.1**)
$FeCl_3$	**−60.5 ± 1.2**;[111] −60.6 ± 1.0[100]	**−60.5**[127] [CCSD(T)-F12b/CBS]; *−59.1*[108] [MP2/CBS]; *−66.8*[139] [est-QCISD(T)/WHext]; *−64.0*[109] [G4(MP2)]
$CoCl_3$	−39.1 ± 2.5[111]	−35.7[128] [CCSD(T)/CBS]; −36.3[127] [CCSD(T)-F12b/CBS]; −35.9[98] [CCSD(T)-DK/CBS]; *−37.6*[109] [G4(MP2)]; *−34.5*[108] [MP2/CBS] (avg: **−36.0**)[f]

[a]All values are in kcal mol^{-1}. [b]Recommended values are given in bold. [c]Level of theory is in square brackets. [CCSD(T)/CBS] denotes the CCSD(T) method in conjunction with Hartree−Fock starting orbitals and CBS extrapolation; in the [CCSD(T)] case, CBS extrapolation has not been performed; [CCSDTQ/CBS] theoretical model includes higher-order excitation terms in correlation as a correction; [CCSD(T)/PW91/CBS] utilizes PW91 DFT functional to produce the starting orbitals for the subsequent CCSD(T) calculations; [BCCD(T)/CBS] is the Brueckner coupled-cluster method, which excludes the single amplitudes from the CCSD wave function via appropriate orbital rotation; [DLPNO−CCSD(T)/CBS] is a local approximation of the canonical CCSD(T), and [DLPNO−CCSD(T1)] uses iterative triples instead of semicanonical ones, while no CBS extrapolation is applied; [CCSD(T)-DK/CBS] utilizes the second-order Douglas−Kroll−Hess Hamiltonian and the all-electron basis sets; explicitly correlated modification of CCSD(T) is denoted as [CCSD(T)-F12b/CBS]; [MP2/CBS] and [G4(MP2)] are composite approaches, based on the MP2 method; [est-QCISD(T)/WHext] refers to a composite approach with the QCISD(T) method and specifically designed WH basis sets within the mentioned work. [d]Average theoretical (DLPNO−)CCSD(T) value is in round brackets, see the main text. Non-CCSD(T) values excluded from averaging are in italic. [e]Derived from $\Delta_{at}H°$ (0 K) with the auxiliary data from ref 100. [f]Uncertainty of 3 kcal mol^{-1} ("transition metal chemical accuracy")[98] was ascribed.

Finally, thermal correction to enthalpy ΔH_{CORR} was calculated within the recently extended[77] msRRHO (τ = 100 cm^{-1}) approximation. These calculations were performed by a series of internally developed Python scripts, available in our GitHub repository.[77] For every considered $M(acac)_3$ complex, an analysis revealed 6 harmonic frequencies that correspond to the internal rotation of the CH_3 groups of the acetylacetonate ligand. To quantify the error associated with our treatment of these modes within the msRRHO(τ = 100 cm^{-1}) approximation, we performed a series of constrained optimizations along the rotation of one CH_3 group in the $Sc(acac)_3$ complex and obtained the corresponding PBE0-D3/def2-TZVP rotational potential. As expected, the potential turned out to be 3-fold with V_0 = 0.6 kcal mol^{-1}. The potential was then used to solve the 1-D hindered rotor Schrodinger equation according to the procedure described in ref 78 and implemented[79] in the *in-house* Python code that is still under development.[53,80] According to the hindered rotor treatment, the enthalpic contribution (ΔH) of each methyl group amounts to ca. 0.5 kcal mol^{-1}. It is on average 0.1 kcal mol^{-1} larger than the msRRHO (τ = 100 cm^{-1}) value of the corresponding vibrational mode. Hence, the error associated with the simplified treatment of the internal rotation of 6 CH_3 groups amounts to ca. 0.7 kcal mol^{-1}.

Based on the previous benchmark studies,[81−83] a few DFT functionals have been considered computationally less

https://doi.org/10.1021/acs.inorgchem.5c03069
Inorg. Chem. 2025, 64, 21405−21418

expensive and sophisticated substitutes of the DLPNO−CCSD(T) method, specifically ωB97M-V,[84] PWPB95-D4,[85−88] and M06-D3(0)[89] with def2-*n*ZVPP (*n* = T and Q) basis sets,[90] followed by CBS extrapolation as described above. The range-separated hybrid meta-GGA ωB97M-V method was employed with the self-consistent nonlocal dispersion correction VV10.[91] The M06 functional from the Minnesota family was used with the zero-damping variant of the D3 dispersion correction.[46] The PWPB95 functional was utilized as implemented in the LibXC library.[92] All single-point DFT calculations and MP2 part of the double-hybrid PWPB95, were sped up with the RIJCOSX approximation.[47,48,93,94]

2.3. Reaction Generator and the Postprocessing Procedure. Enthalpies of reactions were calculated via eq 1. Using the reference experimental enthalpies of formation listed in Table S1 and Table 1 and the predicted enthalpy of reaction, the enthalpy of formation of a target compound can be determined by applying Hess's law. Working reactions are automatically generated and balanced using the reaction generator program (RG), introduced in our previous studies.[32,33] We refer the interested readers to the ref 33 describing the details of the approach and postprocessing procedure. The outline of the key underlying considerations is provided here.

Final enthalpy of formation is a weighted average value. The weights are assigned to the working reactions based on the following characteristics: (1) experimental uncertainties of the reference species; (2) the reaction correlation energy change; and (3) the sum of all reaction stoichiometric coefficients (N) and the absolute difference between the coefficients of products and reagents ($|\Delta N|$). The reaction with the largest weight will be referred to as the "best" reaction.

In order to rule out reactions with large stoichiometric coefficients, the following modification of the original protocol was applied. First, all individual coefficients of the reactants are divided by the coefficient of the target $M(acac)_3$ molecule (c_{targ}). Second, only the reactions with $c_{max}/c_{targ} \leq 10$ (c_{max} is the biggest coefficient in a reaction) are selected for further processing.

The total uncertainty ($u_{95\%}$) assigned to the weighted average enthalpy of formation (see eqs 20 and 22 in the ref 33) accounts for the deviations of the individual $\Delta_f H°$ values from the weighted average as well as for the uncertainties in the reference enthalpies of formation from ATcT. As for the systematic uncertainties of the DLPNO−CCSD(T) method used for the computation of the enthalpies of working reactions ($\Delta_r H°$), those are largely taken into account indirectly due to the error cancellation[95] provided by working reactions. In addition, some portion of the systematic error is also believed to be excluded by averaging over the pool of working reactions. We have refrained from additional efforts to quantitatively estimate the systematic uncertainty, since it requires[96] either a set of well-established experimental data, or very accurate theoretical evaluations for systems of similar size and complexity compared to those of $M(acac)_3$.

3. RESULTS AND DISCUSSION

This section is organized as follows. First, available literature data on the thermochemistry of transition metal reference species and the enol form of acetylacetone are analyzed and discussed. Then, methodological aspects of transition metal tris(acetylacetonates) enthalpies of formation prediction are discussed in Section 3.2, which describes the evaluation of the DLPNO−CCSD(T)/CBS results in comparison with the predictions of DFT methods and their cross-validation through transmetalation reactions. Finally, the critical comparison of experimental and theoretical results is performed in Section 3.3.

3.1. Selection of the Non-ATcT Reference Enthalpies of Formation. The quality of the reaction-based quantum chemical predictions depends on the reliability of the reference species' enthalpies of formation. Accurate enthalpies of formation of relatively simple organic compounds are easily accessible from the ATcT database. Unfortunately, this is not the case for the transition metal reference species, where the discrepancy in the data from different sources may exceed 10 kcal mol^{-1}. In our recent work,[97] we revealed such problematic cases and recommended some experimental and/or computational enthalpies of formation on the basis of the comparison with the CCSD(T)/CBS results.

Table 1 lists the literature-available experimental and theoretical enthalpies of formation of the selected Sc, Ti, V, Cr, Mn, Fe, and Co compounds. Judging between different theoretical approaches, we give preference to the "gold standard" CCSD(T) method. If several CCSD(T)-based $\Delta_f H°$ (g, 298 K) values are available, they were averaged to yield a reference theoretical one. Experimental enthalpies of formation differing by no more than 3 kcal mol^{-1} (so-called transition metal chemical accuracy limit[98]) from the average CCSD(T) values were used as references in the reaction-based FPD approach (Sections 2.2.2 and 2.3) to derive $\Delta_f H°$ (g, 298 K) for $M(acac)_3$ complexes. For several transition metal compounds ($TiOCl_2$, TiF_4, CrO_3, and $CoCl_3$), the literature search reveals no experimental $\Delta_f H°$ (g, 298 K) satisfying the above-mentioned criterion.

We also tried to obtain $\Delta_f H°$ (g, 298 K) of $M(acac)_3$ using the enol form of acetylacetone (Hacac), for which the experimental enthalpy of formation (−90.4 ± 0.3 kcal mol^{-1})[99] was computationally verified in ref 17.

3.2. Reaction-Based Strategies for the Calculation of $M(acac)_3$ Enthalpies of Formation. Enthalpies of formation of $M(acac)_3$ complexes are obtained in this work using specifically constructed model reactions of the type $M(acac)_3$ + A + ⋯ = B + C + ⋯, where A, B, C, etc. are the so-called reference species with accurately known $\Delta_f H°$ (g, 298 K) (Sections 2.1 and 3.1) and enthalpies of reactions are calculated with a chosen electronic structure theory method. This is a well-established error cancellation technique,[19] especially beneficial in the case of sizable molecules. Three different strategies were examined to compose the working reactions. First, our recently introduced reaction generator (RG) program was used, which automatically derives numerous balanced working reactions combining $M(acac)_3$ complexes and user-defined reference species. This approach allows us to generate (potentially) large amounts of independently determined $\Delta_f H°$ (g, 298 K) values, collect some relevant statistics, and eliminate any bias toward particular working reaction(s). Most accurate $\Delta_f H°$ values were calculated using the Feller−Peterson−Dixon (FPD) method and the DLPNO−CCSD(T)/CBS approximation according to eq 1. Computationally cheaper and less sophisticated DFT model chemistries have also been claimed[140] to reach the accuracy comparable to the canonical CCSD(T) method when applied to the 3d-transition metal thermochemistry. To clarify whether it holds for the $M(acac)_3$

https://doi.org/10.1021/acs.inorgchem.5c03069
Inorg. Chem. 2025, 64, 21405−21418

Table 2. Theoretical Gas-Phase Enthalpies of Formation of Transition Metal Complexes with Acetylacetonate Ligand, Derived within the Reaction-Based Feller−Peterson−Dixon Approach with Reaction Generator Results[a]

	$\Delta_fH°$ (g, 298 K)			
"Best" reaction	best reaction value[b]	weighted average value[c]	min/max[d]	SD[e]
$ScC_{15}H_{21}O_6 + O_2 + 3HCl = C_3H_6O + 3C_4H_6O_2 + ScCl_3$	−410.9	−410.2 ± 4.5 [3244]	−419.5/−397.1	2.6
$ScC_{15}H_{21}O_6 + O_2 + 3HF = C_3H_6O_2 + 3C_4H_6O_2 + ScF_3$	−411.5	−410.9 ± 4.8 [5357]	−420.2/−399.0	2.4
$2ScC_{15}H_{21}O_6 + 3O_2 + 2HF = C_2H_2O_4 + 7C_4H_6O_2 + 2ScF$	−413.7	−414.2 ± 4.8 [5170]	−423.0/−401.9	2.2
		−411.5 ± 5.7 [13771]		
$2TiC_{15}H_{21}O_6 + 8HCl = C_2H_2O_4 + 4C_5H_{12} + 8CO + 2TiCl_4$	−375.3	−375.2 ± 3.5 [3354]	−385.0/−362.8	2.5
$10TiC_{15}H_{21}O_6 + 40HF = 11C_2H_4O_2 + 13C_4H_{10} + C_2H_2O + 10TiF_4$	*−369.1*	*−368.0 ± 3.1* [4945]	*−377.6/−355.2*	2.3
$2TiC_{15}H_{21}O_6 + 6H_2 = 2C_5H_{12} + 3C_4H_6O_2 + 2TiO$	−369.8	−370.3 ± 4.2 [1001]	−377.4/−358.0	2.3
$8TiC_{15}H_{21}O_6 + 36H_2O = 19O_2 + 30C_4H_8O + 8TiO_2$	−372.5	−369.9 ± 6.5 [921]	−376.8/−359.0	2.4
$6TiC_{15}H_{21}O_6 + 11H_2 + 12HCl = 20C_4H_8O + 10CO + 6TiOCl_2$	*−368.3*	*−369.6 ± 4.8* [3118]	*−379.6/−357.6*	2.4
		−374.8 ± 4.5 [5276]		
$8C_{15}H_{21}O_6 + 13H_2O = 7C_4H_8O + 23C_4H_6O_2 + 8VO$	−336.3	−335.6 ± 4.2 [1001]	−342.6/−323.3	2.3
$8VC_{15}H_{21}O_6 + 36H_2O = 19O_2 + 30C_4H_8O + 8VO_2$	−342.2	−339.6 ± 5.2 [921]	−346.5/−328.7	2.4
		−335.8 ± 4.7 [1922]		
$2CrC_{15}H_{21}O_6 + 3O_2 + 2HCl = C_2H_2O_4 + 7C_4H_6O_2 + 2CrCl$	−328.4	−328.8 ± 4.1 [3666]	−337.8/−316.5	2.5
$2CrC_{15}H_{21}O_6 + 6H_2 = 2C_5H_{12} + 5O_2C_4H_6 + 2CrO$	−329.6	−330.1 ± 10.7 [1001]	−337.2/−317.9	2.3
$8CrC_{15}H_{21}O_6 + 36H_2O = 15O_2 + 30OC_4H_8 + 8CrO_3$	*−327.2*	*−324.8 ± 5.1* [840]	*−332.3/−313.7*	2.5
		−328.8 ± 4.2 [4667]		
$2MnC_{15}H_{21}O_6 + 7O_2 + 2ClOCH = 4C_2H_2O_4 + 6O_2C_4H_6 + 2MnCl$	−285.9	−289.1 ± 4.2 [3666]	−298.1/−276.8	2.4
$2MnC_{15}H_{21}O_6 + 3O_2 + 4CH_3Cl = 2C_3H_6O_2 + 7C_4H_6O_2 + 2MnCl_2$	−291.9	−292.1 ± 3.6 [3443]	−301.8/−280.8	2.4
$8MnC_{15}H_{21}O_6 + 29O_2 + 2CF_4 = 15C_2H_2O_4 + 23C_4H_6O_2 + 8MnF$	−287.1	−290.1 ± 4.7 [5170]	−299.0/−277.9	2.2
		−291.2 ± 4.7 [12279]		
$3FeC_{15}H_{21}O_6 + 3O_2 + 3HCl = 11C_4H_6O_2 + 3FeCl + 2CO_2$	−281.5	−281.6 ± 4.7 [3666]	−290.5/−269.2	2.4
$10FeC_{15}H_{21}O_6 + 20HCl = 22C_2H_2O + 6C_5H_{12} + 19C_4H_6O_2 + 10FeCl_2$	−281.2	−280.5 ± 3.5 [3443]	−290.1/−269.1	2.4
$5FeC_{15}H_{21}O_6 + 15CH_3Cl = 12C_2H_2O + 6C_5H_{12} + 9O_2C_4H_6 + 5FeCl_3$	−286.8	−285.7 ± 4.0 [3244]	−294.9/−272.6	2.6
		−282.5 ± 6.2 [10353]		
$CoC_{15}H_{21}O_6 + 2O_2 + 3CH_3Cl = 2C_3H_6O_2 + 3C_4H_6O_2 + CoCl_3$	−266.5	**−267.6 ± 5.3** [3244]	−277.0/−254.7	2.6

[a]All values are in kcal mol^{-1}. [b]Best reactions were determined as described in Section 2.3, see also ref 33. [c]Average values calculated for the combined sets of reactions are given in bold. Enthalpies of formation excluded from the averaging are given in italic. Numbers of reactions are given in square brackets. [d]Minimum and maximum $\Delta_fH°$ (g, 298 K) values in the sets. [e]Standard deviation for the set of computed $\Delta_fH°$ (g, 298 K).

complexes, we also computed reaction enthalpies using several DFT methods.

Second, the computed DLPNO−CCSD(T)-based $\Delta_fH°$ (g, 298 K) values were cross-validated to check their internal consistency using transmetalation reactions, i.e., the enthalpy of formation of each $M(acac)_3$ was derived through the working reactions with other complexes used as reference compounds.

Finally, additional working reactions with the non-ATcT Hacac molecule, which are expected to ensure the most pronounced error compensation, were constructed for each $M(acac)_3$ complex. The corresponding reaction enthalpies were calculated by using both DLPNO−CCSD(T)/CBS (eq 1) and DFT protocols.

3.2.1. Enthalpies of the Formation of M(acac)$_3$ Obtained with the Reaction Generator. The enthalpies of formation of the target $M(acac)_3$ complexes were derived in automatic mode using the reaction generator (RG) program (see Section 2.3). Each program run required a list of the user-defined reference compounds, utilized as reactants in the generated working reactions. The major part of this list was the same for all $M(acac)_3$ complexes and included simple compounds from the ATcT database (see Table S1). Different transition metal (TM) species were used in the independent RG runs along with additional F- and Cl-containing ATcT compounds to balance the working reactions. Depending on a $M(acac)_3$ complex and a TM reference, 840−5357 reactions were automatically composed and balanced (Table 2). It is evident that the $\Delta_fH°$ (g, 298 K) value predicted using the reaction-based approach depends on the reaction utilized for its derivation due to the limited accuracy of the reference $\Delta_fH°$ (g, 298 K) and calculated $\Delta_rH°$. An inspection of Table 2 indicates that the typical spread in $\Delta_fH°$ (g, 298 K) of $M(acac)_3$ is about 21 kcal mol^{-1}. This large discrepancy is mainly due to the few inappropriate reactions possessing low weights (see Section 2.3) and practically not contributing to the weighted average $\Delta_fH°$ (g, 298 K). At the same time, the overall $\Delta_fH°$ (g, 298 K) distributions are quite narrow as reflected by small standard deviations (Table 2, column 5) and reinforce the robustness of the predicted enthalpies of formation of $M(acac)_3$.

Turning to the comparison of the average $\Delta_fH°$ (g, 298 K) values obtained for each $M(acac)_3$ using different TM references, the most consistent results (deviations less than 3 kcal mol^{-1}) were found for the complexes of Cr and Mn. Somewhat worse agreement between average $\Delta_fH°$(g, 298 K) was detected for the other tris(acetylacetonates), but the values are still within the estimated error limits. Note that in the case of $Ti(acac)_3$, using TiF_4 and $TiOCl_2$ species as references resulted in a larger (up to 6.8 kcal mol^{-1}) deviation from the final average $\Delta_fH°$ (g, 298 K) value of −374.8 kcal mol^{-1}. Both TM compounds exhibited the most pronounced discrepancies

https://doi.org/10.1021/acs.inorgchem.5c03069
Inorg. Chem. 2025, 64, 21405−21418

Table 3. Theoretical Gas-Phase Enthalpies of Formation of Transition Metal Complexes, Derived within the Reaction-Based Approach with Reaction Generator and ωB97M-V/CBS, PWPB95-D4/CBS, and M06-D3(0)/CBS Functional Results[a]

	$\Delta_f H°$ (g, 298 K)			
	best reaction value[b]	weighted average value[c]	min-max[d]	SD[e]
	ωB97M-V/CBS	ωB97M-V/CBS	ωB97M-V/CBS	ωB97M-V/CBS
	PWPB95-D4/CBS	PWPB95-D4/CBS	PWPB95-D4/CBS	PWPB95-D4/CBS
"Best" reaction	M06-D3(0)/CBS	M06-D3(0)/CBS	M06-D3(0)/CBS	M06-D3(0)/CBS
	−409.8	−410.1 ± 5.5	−429.4/−391.4	3.5
$5ScC_{15}H_{21}O_6 + 15HCl = 6C_2H_2O + 3C_5H_{12} + 12C_4H_6O_2 + 5ScCl_3$	−410.7	−412.2 ± 9.5	−443.2/−386.3	6.6
	−401.9	404.3 ± 21.8	−474.9/−342.3	14.3
	−411.0	−411.0 ± 6.7	−432.8/−394.0	4.0
$5ScC_{15}H_{21}O_6 + 8H_2 + 5HF = 3C_5H_{12} + 15C_4H_6O_2 + 5ScF$	−417.1	−416.7 ± 10.5	−449.0/−393.7	6.9
	−416.0	−412.6 ± 22.9	−477.9/−345.5	14.6
	−410.0	−412.1 ± 7.3	−433.4/−391.2	4.1
$5ScC_{15}H_{21}O_6 + 3H_2 + 15HF = 3C_5H_{12} + 15C_4H_6O_2 + 5ScF_3$	−412.9	−414.3 ± 10.8	−446.4/−387.1	7.0
	−416.4	−415.1 ± 23.1	−486.9/−352.3	14.7
		−411.1 ± 6.7		
		−414.2 ± 10.9		
		−410.2 ± 24.4		
	−386.0	−386.0 ± 4.6	−404.5/−361.7	3.3
$10TiC_{15}H_{21}O_6 + 19H_2 + 40HCl = 24C_5H_{12} + 30CO_2 + 10TiCl_4$	−374.3	−376.1 ± 9.4	−406.6/−350.1	6.3
	−351.2	−365.0 ± 21.7	−438.5/−303.8	13.9
	−376.9	−376.5 ± 5.4	−397.5/−364.0	3.5
$2TiC_{15}H_{21}O_6 + 6H_2 = 2C_5H_{12} + 5C_4H_6O_2 + 2TiO$	−375.2	−373.4 ± 9.5	−404.7/−351.0	7.0
	−389.6	−384.3 ± 22.8	−443.7/−319.4	15.2
	−384.0	−383.9 ± 7.3	−405.3/−371.5	3.4
$10TiC_{15}H_{21}O_6 + 39H_2 = 14C_5H_{12} + 20C_4H_6O_2 + 10TiO_2$	−376.0	−374.1 ± 9.7	−406.6/−358.0	5.9
	−382.8	−378.3 ± 21.2	−430.2/−311.5	13.7
	−374.5	*−373.4 ± 7.3*	*−398.0*/−350.3	4.3
$10TiC_{15}H_{21}O_6 + 19H_2 + 40HF = 24C_5H_{12} + 30CO_2 + 10TiF_4$	−369.4	*−372.2 ± 12.0*	*−406.3*/−346.1	7.0
	−358.5	*−370.8 ± 26.0*	*−448.4*/−311.1	14.6
	−382.9	−382.6 ± 5.6	*−402.2*/−362.7	3.3
$2TiC_{15}H_{21}O_6 + 4H_2 + 4HCl = 2C_5H_{12} + 5C_4H_6O_2 + 2TiOCl_2$	−376.6	*−375.9 ± 9.7-*	*−408.1*/−350.3	6.5
	−377.5	*375.1 ± 22.3*	*−437.5*/−310.6	14.2
		−381.8 ± 5.5		
		−375.9 ± 9.6		
		−366.5 ± 24.0		
	−345.5	−345.2 ± 5.3	−366.1/−332.7	3.5
$2VC_{15}H_{21}O_6 + 6H_2 = 2C_5H_{12} + 5C_4H_6O_2 + 2VO$	−345.1	−343.3 ± 9.4	−374.6/−321.0	7.0
	−345.2	−339.9 ± 22.8	−399.3/−275.0	15.2
	−355.8	−355.7 ± 6.1	−377.1/−343.3	3.4
$10VC_{15}H_{21}O_6 + 39H_2 = 14C_5H_{12} + 20C_4H_6O_2 + 10VO_2$	−346.0	−344.1 ± 8.8	−376.6/−328.0	5.9
	−354.4	−349.9 ± 20.9	−401.8/−283.1	13.7
		−348 ± 10.8		
		−343.5 ± 9.3		
		−342.5 ± 24.0		
	−321.5	−321.8 ± 5.1	−342.5/−305.1	3.4
$4CrC_{15}H_{21}O_6 + 7H_2 + 4HCl = 6C_4H_8O + 9C_4H_6O_2 + 4CrCl$	−332.4	−332.0 ± 9.8	−362.2/−308.0	6.6
	−324.2	−321.4 ± 22.7	−386.2/−254.5	14.3
	−338.0	−337.7 ± 11.2	−358.6/−325.1	3.5
$2CrC_{15}H_{21}O_6 + 6H_2 = 2C_5H_{12} + 5C_4H_6O_2 + 2CrO$	−344.7	−342.9 ± 13.6	−374.2/−320.5	7.0
	−341.7	−336.7 ± 24.5	−395.9/−271.6	15.2
	−363.2	*−364.9 ± 6.6*	*−386.7*/−352.6	3.7
$4CrC_{15}H_{21}O_6 + 13H_2O = 5C_4H_{10}O + 10C_4H_6O_2 + 4CrO_3$	−332.3	*−335.0 ± 9.1*	*−362.5*/−314.1	6.2
	−350.4	*−353.2 ± 22.3*	*−413.6*/−285.8	14.5
		−321.9 ± 6.0		
		−332.1 ± 10.1		
	−301.6	−301.8 ± 5.2	−322.5/−285.1	3.4
$4MnC_{15}H_{21}O_6 + 7H_2 + 4HCl = 6C_4H_8O + 9C_4H_6O_2 + 4MnCl$	−305.8	−305.4 ± 9.8	−335.6/−281.4	6.6
	−312.3	−309.5 ± 22.6	−374.2/−242.6	14.3

https://doi.org/10.1021/acs.inorgchem.5c03069
Inorg. Chem. 2025, 64, 21405−21418

Table 3. continued

"Best" reaction	$\Delta_f H°$ (g, 298 K) best reaction value[b] ωB97M-V/CBS PWPB95-D4/CBS M06-D3(0)/CBS	$\Delta_f H°$ (g, 298 K) weighted average value[c] ωB97M-V/CBS PWPB95-D4/CBS M06-D3(0)/CBS	$\Delta_f H°$ (g, 298 K) min-max[d] ωB97M-V/CBS PWPB95-D4/CBS M06-D3(0)/CBS	$\Delta_f H°$ (g, 298 K) SD[e] ωB97M-V/CBS PWPB95-D4/CBS M06-D3(0)/CBS
	−301.4	−301.7 ± 4.7	−322.7/−281.5	3.3
$10MnC_{15}H_{21}O_6 + 20HCl = 22C_2H_2O + 6C_5H_{12} + 19C_4H_6O_2 + 10MnCl_2$	−304.0	−306.3 ± 9.8	−338.2/−281.8	6.5
	−299.5	−305.2 ± 22.5	−372.6/−242.0	14.1
$5MnC_{15}H_{21}O_6 + 8H_2 + 5HF = 3C_5H_{12} + 15C_4H_6O_2 + 5MnF$	−300.8	−301.0 ± 6.6	−322.6/−283.7	4.0
	−305.1	−304.7 ± 10.4	−337.0/−281.7	6.9
	−315.1	−311.6 ± 22.9	−377.0/−244.5	
		−301.7 ± 5.1		
		−305.8 ± 10.0		
		−307.3 ± 23.1		
	−284.8	−284.6 ± 5.7	−305.3/−267.9	3.4
$5FeC_{15}H_{21}O_6 + 8H_2 + 5HCl = 3C_5H_{12} + 15C_4H_6O_2 + 5FeCl$	−287.6	−287.0 ± 10.0	−317.2/−263.0	6.6
	−302.5	−299.1 ± 22.5	−363.7/−232.1	14.3
	−278.6	−279.0 ± 4.7	−299.9/−258.8	3.3
$10FeC_{15}H_{21}O_6 + 20HCl = 22C_2H_2O + 6C_5H_{12} + 19C_4H_6O_2 + 10FeCl_2$	−281.1	−283.3 ± 9.8	−315.3/−258.8	6.5
	−283.0	−288.6 ± 22.5	−356.0/−225.5	14.1
	−287.9	−288.2 ± 5.2	−307.5/−269.5	3.5
$5FeC_{15}H_{21}O_6 + 15HCl = 6C_2H_2O + 3C_5H_{12} + 12C_4H_6O_2 + 5FeCl_3$	−289.1	−290.5 ± 9.5	−321.6/−264.7	6.6
	−278.3	−280.5 ± 22.0	−351.3/−218.7	14.3
		−282.8 ± 9.9		
		−286.3 ± 11.8		
		−286.8 ± 24.9		
	−272.1	**−272.0 ± 5.9**	−291.3/−253.3	3.5
$5CoC_{15}H_{21}O_6 + 3H_2 + 15HCl = 3C_5H_{12} + 15C_4H_6O_2 + 5CoCl_3$	−277.1	**−277.2 ± 9.7**	−308.3/−251.3	6.6
	−254.7	**−252.8 ± 21.8**	−323.3/−190.7	14.3

[a]All values are in kcal mol^{-1}. [b]Best reactions were determined as described in Section 2.3, see also ref 33 [c]Average values calculated for the combined sets of reactions are given in bold. Enthalpies of formation excluded from the averaging are given in italic. The number of reactions is the same as that for the DLPNO−CCSD(T)/CBS method (see Table 2, column 3). [d]Minimum and maximum $\Delta_f H°$ (g, 298 K) values in the sets. [e]Standard deviation for the set of computed $\Delta_f H°$ (g, 298 K).

in their theoretical and experimental enthalpies of formation (Section 3.1).

For illustration purposes, the best reactions possessing the largest weights are also listed in Table 2 (column 1). In some cases, differences between the enthalpies of formation derived from the best reactions and their weighted average counterparts are more than 3 kcal mol^{-1}. It implies that one cannot rely on a single (even seemingly "good") reaction to derive a robust $\Delta_f H°$ (g, 298 K).

We also examined an appealing replacement of the costly DLPNO−CCSD(T) $\Delta_r H°$ calculations with cheaper DFT model chemistries (Table 3). Depending on a particular DFT approximation, average standard deviations (SDs) reflecting the spread of $\Delta_f H°$ (g, 298 K) values within the sets of generated reactions are 3.6 kcal mol^{-1} (ωB97M-V), 6.6 kcal mol^{-1} (PWPB95-D4), and 14.4 kcal mol^{-1} (M06-D3(0)). The analogous average SD value for the DLPNO−CCSD(T) method is approximately 2.4 kcal mol^{-1}. In other words, DFT-based enthalpies of formation are less consistent with each other, and larger uncertainty is introduced into the final weighted average $\Delta_f H°$ (g, 298 K).

3.2.2. M(acac)$_3$ Enthalpies of Formation Derived from Transmetalation Reactions. In order to check the internal consistency of the predicted enthalpies of formation, transmetalation reactions containing simultaneously two different M(acac)$_3$ complexes were constructed. Appropriate TM reference species and several small inorganic compounds (H_2, H_2O, HCl, and HF) were used as balancing reactants in the working reactions. The obtained values (Table 4, column 2) are in excellent agreement with the final theoretical enthalpies of formation (Table 2). The latter set of values is

Table 4. Enthalpies of Formation Based on the Transmetalation Reactions and DLPNO−CCSD(T)/CBS Calculations[a]

M(acac)$_3$	$\Delta_f H°$ (g, 298 K), transmetalation	min/max[b]	SD[c]	Δ[d]
Sc(acac)$_3$	−413.2 ± 8.6	−417.8/−407.1	2.8	1.7
Ti(acac)$_3$	−372.0 ± 8.8	−378.6/−366.5	3.4	2.8
V(acac)$_3$	−337.4 ± 8.9	−343.3/−331.8	3.3	1.6
Cr(acac)$_3$	−329.6 ± 8.2	−333.2/−324.9	2.5	0.8
Mn(acac)$_3$	−290.8 ± 7.8	−295.3/−285.2	2.7	0.4
Fe(acac)$_3$	−282.7 ± 8.0	−289.3/−276.8	3.4	0.2
Co(acac)$_3$	−268.8 ± 7.1	−271.4/−265.3	2.1	1.2

[a]All values are in kcal mol^{-1}. [b]Minimum and maximum $\Delta_f H°$ (g, 298 K) values in the sets. [c]Standard deviation for the set of computed $\Delta_f H°$ (g, 298 K). [d]The difference between $\Delta_f H°$ (g, 298 K) obtained using transmetalation reactions and final RG value (Table 2, column 3).

https://doi.org/10.1021/acs.inorgchem.5c03069
Inorg. Chem. 2025, 64, 21405−21418

Table 5. Enthalpies of Formation of $M(acac)_3$ Complexes According to DLPNO−CCSD(T) and DFT Approximations[a,b,c]

reaction	$\Delta_f H°$ (g, 298 K) DLPNO−CCSD(T)	PWPB95-D4	ωB97M-V	M06-D3(0)
$Sc(acac)_3 + 3HCl = ScCl_3 + 3Hacac$	−411.1 ± 0.8	−407.7 ± 0.8	−407.7 ± 0.8	−404.9 ± 0.8
$Sc(acac)_3 + H_2 + HF = ScF + 3Hacac$	−414.2 ± 0.9	−412.7 ± 0.9	−408.5 ± 0.9	−414.6 ± 0.9
$Sc(acac)_3 + 3HF = ScF_3 + 3Hacac$	−410.8 ± 1.1	−407.6 ± 1.1	−406.5 ± 1.1	−414.0 ± 1.1
	−411.1 ± 5.0	**−409.4 ± 7.4**	**−407.1 ± 3.0**	**−411.2 ± 13.6**
$Ti(acac)_3 + 4HCl = 1/2H_2 + TiCl_4 + 3Hacac$	−376.1 ± 0.3	−371.4 ± 0.3	−379.9 ± 0.3	−364.8 ± 0.3
$Ti(acac)_3 + 1/2H_2 + H_2O = TiO + 3Hacac$	−370.5 ± 0.6	−369.6 ± 0.6	−374.3 ± 0.6	−386.1 ± 0.6
$Ti(acac)_3 + 2H_2O = 1/2H_2 + TiO_2 + 3Hacac$	−370.8 ± 1.4	−369.3 ± 1.4	−381.4 ± 1.4	−377.4 ± 1.4
$Ti(acac)_3 + 4HF = 1/2H_2 + TiF_4 + 3Hacac$	*−368.7 ± 0.2*	*−366.4 ± 0.2*	*−368.4 ± 0.2*	*−372.1 ± 0.2*
$Ti(acac)_3 + H_2O + 2HCl = 1/2H_2 + TiOCl_2 + 3Hacac$	*−370.7 ± 0.7*	*−371.0 ± 0.7*	*−380.3 ± 0.7*	*−374.0 ± 0.7*
	−372.5 ± 8.0	**−369.2 ± 3.2**	**−380.7 ± 9.4**	**−375.1 ± 17.7**
$V(acac)_3 + 1/2H_2 + H_2O = VO + 3Hacac$	−335.7 ± 0.6	−339.6 ± 0.6	−342.9 ± 0.6	−341.8 ± 0.6
$V(acac)_3 + 2H_2O = 1/2H_2 + VO_2 + 3Hacac$	−340.5 ± 0.9	−339.3 ± 0.9	−353.2 ± 0.9	−349.0 ± 0.9
	−336.7 ± 30.2	**−339.4 ± 2.2**	**−348.1 ± 65.0**	**−345.4 ± 45.9**
$Cr(acac)_3 + HCl + H_2 = CrCl + 3Hacac$	−328.9 ± 0.5	−328.2 ± 0.5	−319.4 ± 0.5	−323.5 ± 0.5
$Cr(acac)_3 + 1/2H_2 + H_2O = CrO + 3Hacac$	−330.4 ± 2.6	−339.1 ± 2.6	−335.4 ± 2.6	−338.3 ± 2.6
$Cr(acac)_3 + 3H_2O = 3/2H_2 + CrO_3 + 3Hacac$	*−326.4 ± 0.9*	*−329.2 ± 0.9*	*−362.0 ± 0.9*	*−350.9 ± 0.9*
	−329.6 ± 10.0	**−333.7 ± 69.3**	**−327.4 ± 101.5**	**−330.9 ± 93.9**
$Mn(acac)_3 + HCl + H_2 = MnCl + 3Hacac$	−289.2 ± 0.5	−301.6 ± 0.5	−299.4 ± 0.5	−311.5 ± 0.5
$Mn(acac)_3 + 1/2H_2 + 2HCl = MnCl_2 + 3Hacac$	−292.5 ± 0.3	−302.2 ± 0.3	−299.5 ± 0.3	−306.2 ± 0.3
$Mn(acac)_3 + H_2 + HF = MnF + 3Hacac$	−290.2 ± 0.8	−300.7 ± 0.8	−298.2 ± 0.8	−313.6 ± 0.8
	−290.6 ± 4.3	**−301.4 ± 2.1**	**−299.0 ± 1.8**	**−309.9 ± 9.5**
$Fe(acac)_3 + H_2 + HCl = FeCl + 3Hacac$	−281.6 ± 0.5	−283.2 ± 0.5	−282.2 ± 0.5	−301.0 ± 0.5
$Fe(acac)_3 + 3HCl = FeCl_3 + 3Hacac$	−286.5 ± 0.8	−286.2 ± 0.8	−285.8 ± 0.8	−281.4 ± 0.8
$Fe(acac)_3 + 1/2H_2 + 2HCl = FeCl_2 + 3Hacac$	−280.8 ± 0.3	−279.2 ± 0.3	−276.8 ± 0.3	−289.7 ± 0.3
	−283.0 ± 7.8	**−282.9 ± 8.7**	**−281.6 ± 11.3**	**−290.7 ± 24.6**
$Co(acac)_3 + 3HCl = CoCl_3 + 3Hacac$	**−271.7 ± 1.1**	**−275.9 ± 1.1**	**−272.6 ± 1.1**	**−256.4 ± 1.1**
MUD		4.1	5.6	10.0
maximum deviation		12.4	12.8	23.4

[a]All values are in kcal mol^{-1}. [b]Values in bold are averages over all reactions for each $M(acac)_3$ complex. Uncertainties are estimated as $u = \sqrt{u_{Student}^2 + u_{exp}^2}$, where $u_{Student}$ is Student's expanded uncertainty (confidence level 95%) and u_{exp} is uncertainty due to enthalpies of formation of reference species (see eq 11 in ref 33). [c]Values in italic are considered to be less reliable and are excluded from the averaging.

further used for the validation of the experimental enthalpies of formation of the studied complexes.

3.2.3. $M(acac)_3$ Enthalpies of Formation Derived from Reactions with Hacac. In this section, we will separately consider the working reactions with the Hacac molecule taken as a reference (see Table 5). Such reactions are expected to be beneficial from the point of view of error compensation. The obtained average $\Delta_f H°$ (g, 298 K) values (Table 5, column 2) in most cases are within 1 kcal mol^{-1} with their RG weighted average counterparts (Table 2, column 3), except for $Ti(acac)_3$ (2.3 kcal mol^{-1}) and $Co(acac)_3$ (4.1 kcal mol^{-1}).

To assess the influence of the theory level on the derived $\Delta_f H°$ (g, 298 K) of $M(acac)_3$, we also performed additional DFT calculations. The best agreement with the DLPNO−CCSD(T) results was found for the double-hybrid PWPB95-D4 functional (MUD = 4.1 kcal mol^{-1}), followed by ωB97M-V (MUD = 5.6 kcal mol^{-1}), see also Figure 1. The M06 functional complemented by D3(0) dispersion correction demonstrated worse performance with MUD = 10.0 kcal mol^{-1}. Deviations of similar magnitude were previously found for the complexes of transition metals with tetraphenylporphyrine.[35]

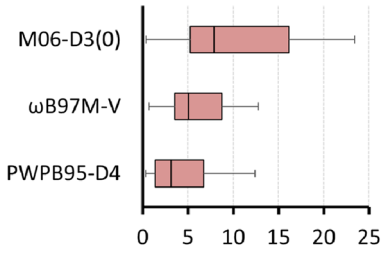

Figure 1. Deviations of DFT-based enthalpies of formation of $M(acac)_3$ complexes obtained using the working reactions with Hacac from their reference DLPNO−CCSD(T)/CBS counterparts. The left and right sides of the boxes correspond to the first (Q_1) and third (Q_3) quartiles, respectively. The vertical solid line inside each box gives the median deviation. The whiskers give the lowest and largest deviations for each method. All values are in kcal mol^{-1}.

3.3. Rationalization of the Literature-Available Enthalpies of Formation and Sublimation of $M(acac)_3$ Complexes. Finally, the predicted theoretical enthalpies of formation are compared with their literature-available experimental counterparts (Table 6). Experimental gas-phase $\Delta_f H°$ (g, 298 K) values were obtained by summing the corresponding solid-state $\Delta_f H°$ (g, 298 K) and sublimation

https://doi.org/10.1021/acs.inorgchem.5c03069
Inorg. Chem. 2025, 64, 21405−21418

Table 6. Theoretical and Experimental Enthalpies of Formation of $M(acac)_3$ Complexes[a]

	$\Delta_fH°$ (g, 298 K)[c]	$\Delta_fH°$ (g, 298 K)[b]
$M(acac)_3$	theory, this work	Expt.
$Sc(acac)_3$	−411.5 ± 5.7	*−398.4 ± 3.6* [*−424.5 ± 3.6*[141] + 30.2 ± 0.3[18]]
$Ti(acac)_3$	−374.8 ± 4.5	
$V(acac)_3$	−335.8 ± 4.7	−334.6 ± 1.3 [−364.0 ± 1.1[143] + 29.4 ± 0.7[143]]; *−364.7 ± 7.2* [*−394.1 ± 7.2*[141] + 29.4 ± 0.7[18]]
$Cr(acac)_3$	−328.8 ± 4.2	−343.0 ± 2.2 [−374.0 ± 2.1[146] + 31.0 ± 0.7[18]]; −335.5 ± 0.7 [−366.5 ± 0.7[147] + 31.0 ± 0.2[18]]; *−322.7 ± 3.3* [*−353.7 ± 3.3*[141] + 31.0 ± 0.2[18]]
$Mn(acac)_3$	−291.2 ± 4.7	−298.2 ± 1.1 [−329.6 ± 0.9[144] + 31.4 ± 0.7[18]]; *−293.7 ± 3.0* [*−325.1 ± 2.9*[141] + 31.4 ± 0.7[18]]
$Fe(acac)_3$	−282.5 ± 6.2; (−282.5 ± 1.0[e])	−282.8 ± 0.8 [−314.2 ± 0.7[d] + 31 ± 0.4[18]]; *−324.2 ± 3.6* [*−355.2 ± 3.6*[141] + 31 ± 0.4[18]]
$Co(acac)_3$	−267.6 ± 5.3	−264.0 ± 1.1 [−294.9 ± 0.9[145] + 30.9 ± 0.6[18]]; *−295.3 ± 4.3* [*−326.2 ± 4.3*[141] + 30.9 ± 0.6[18]]

[a]All values are in kcal mol^{-1}. [b]Values of questionable accuracy are in italics. [c]Theoretical enthalpy of formation is obtained using the reaction generator (Section 3.2.1). [d]Weighted mean value from ref 17. [e]Theoretical value obtained using the DLPNO−CCSD(T)/CBS Feller−Peterson−Dixon reaction-based approach in ref 17.

enthalpies. The latter values (except for $V(acac)_3$) were derived[18] by Zherikova and co-workers on the basis of the careful inspection of the literature data. It should be noted that the accuracy of the early determinations of $\Delta_fH°$ (g, 298 K) reported by Wood and Jones (WJ)[141] was further questioned by Ribeiro da Silva.[142] This can be a reason for the 13.1 kcal mol^{-1} disagreement between experimental and theoretical $\Delta_fH°$ (g, 298 K) values for $Sc(acac)_3$. For $V(acac)_3$, our predicted $\Delta_fH°$ (g, 298 K) is within the estimated error limits with the experimental value by Jamea and Pilcher[143] and is in strong disagreement (28.9 kcal mol^{-1}) with the result of WJ.[141] In the case of $Cr(acac)_3$, three independent $\Delta_fH°$ (g, 298 K) measurements have been carried out, and the obtained values are not in agreement with each other. Theoretical enthalpy of formation of $Cr(acac)_3$ does not provide support for any experimental value, and additional measurements are recommended. In case of $Mn(acac)_3$, the predicted $\Delta_fH°$ (g, 298 K) surprisingly is within the error limits with the result obtained using $\Delta_fH°$ (g, 298 K) by WJ[141] and does not support the more recent value reported in ref 144. Detailed rationalization of the experimental enthalpies of formation of $Fe(acac)_3$ was performed in our previous study.[17] Here, we need only mention that the updated theoretical value of $\Delta_fH°$ (g, 298 K) = −282.5 ± 6.2 kcal mol^{-1} perfectly meets the older result (−282.5 ± 1.0 kcal mol^{-1}) obtained using a slightly different FPD protocol and original implementation of the RG program. Larger uncertainty of $\Delta_fH°$ (g, 298 K) in this work is related to the significant extension of the list of reference species and, in turn, working reactions used for the derivation of the weighted average enthalpy of formation. We believe that this updated uncertainty is also more realistic, taking into account the size and complexity of the studied system and inherent errors of the reaction-based approach stemming from the limited accuracy of reference $\Delta_fH°$ (g, 298 K) and theoretical enthalpies of working reactions. Finally, our predicted $\Delta_fH°$ (g, 298 K) for $Co(acac)_3$ is within the error limits with the experimental data obtained as a combination of $\Delta_fH°$ (cr, 298 K) determined[145] by Ribeiro da Silva and $\Delta_{sub}H°$ (g, 298 K) from ref 18. No experimental data were found for $Ti(acac)_3$, and the corresponding investigations could shed further light on the accuracy of the computational protocol used in this work.

4. CONCLUSIONS

The gas-phase enthalpies of formation ($\Delta_fH°$ (g, 298 K)) of Sc, Ti, V, Cr, Mn, Fe, and Co tris(acetylacetonates) were obtained using the DLPNO−CCSD(T)/CBS Feller−Peterson-Dixon (FPD) approach and the recently developed program for the generation of working reactions. The reactions were automatically composed using some simple compounds for which accurate enthalpies of formation are documented in the ATcT database and the corresponding transition metal oxides, fluorides, and chlorides. A careful analysis of the literature-available experimental and theoretical enthalpies of formation of the transition metal references was performed to establish their reliable $\Delta_fH°$ (g, 298 K) values. The predicted enthalpies of formation of $M(acac)_3$ complexes were cross-validated to check the internal consistency. Using the cheaper DFT approximations instead of the sophisticated DLPNO−CCSD(T) FPD protocol results in the more pronounced dependence of the $\Delta_fH°$ (g, 298 K) value on a particular reaction and increased uncertainties in the final enthalpies of formation.

Final theoretical $\Delta_fH°$ (g, 298 K) values of $M(acac)_3$ were utilized for the verification of their counterparts computed from the previously reported solid-state enthalpies of formation ($\Delta_fH°$ (cr, 298 K)) and sublimation enthalpies. In the case of $V(acac)_3$, $Fe(acac)_3$, and $Co(acac)_3$, our predicted $\Delta_fH°$ (g, 298 K) are within the error limits with the corresponding experimental values. For $Mn(acac)_3$, the theoretical $\Delta_fH°$ (g, 298 K) better agrees with the value derived on the basis of the respective solid-state value from the seminal study of Wood and Jones,[141] whose results have been called into question in further studies. The gas-phase enthalpy of formation of $Sc(acac)_3$ does not support the experimental value, with a difference of 13.1 kcal mol^{-1}. In the case of $Cr(acac)_3$, theoretical $\Delta_fH°$ (g, 298 K) lies between two experimental values, with deviations of 6.1 and 6.7 kcal mol^{-1}, respectively. To the best of our knowledge, no experimental data on the enthalpies of formation of $Ti(acac)_3$ have been reported to date. Further experimental studies could not only fill this gap but also provide an additional independent assessment of the computational protocol applied in this work.

■ ASSOCIATED CONTENT

Data Availability Statement

Cartesian coordinates (in Å) of PBE0-D3(BJ)/def2-TZVP optimized structures along with harmonic frequencies in the form of *dat files used for the calculations of the thermal correction to enthalpy H_{CORR} with the standalone thermochemistry program, tabulated DLPNO−CCSD(T) and DFT single-point energies, and T_1/t_2 diagnostics values in the form

https://doi.org/10.1021/acs.inorgchem.5c03069
Inorg. Chem. 2025, 64, 21405−21418

of *txt files for all $M(acac)_3$ complexes and reference species. (https://github.com/QuantumChemistryGroup/Macac3/tree/main/SI).

Supporting Information

The Supporting Information is available free of charge at https://pubs.acs.org/doi/10.1021/acs.inorgchem.5c03069.

Reference enthalpies of formation of ATcT species; energies of spin-state splittings for some of the $M(acac)_3$ complexes; reaction enthalpies from Table 2 with contributions within the FPD approach; absolute deviations of reaction energies obtained with DFT methods compared to those from the DLPNO−CCSD(T)/CBS protocol; and total entropies of the transition metal tris(acetylacetonates) (PDF)

AUTHOR INFORMATION

Corresponding Author

Yury Minenkov − *N.N. Semenov Federal Research Center for Chemical Physics RAS, 119991 Moscow, Russian Federation;* orcid.org/0000-0001-8993-056X; Email: Yury.Minenkov@chph.ras.ru

Authors

Andrey D. Moshchenkov − *N.N. Semenov Federal Research Center for Chemical Physics RAS, 119991 Moscow, Russian Federation*

Alexander S. Ryzhako − *N.N. Semenov Federal Research Center for Chemical Physics RAS, 119991 Moscow, Russian Federation*

Arseniy A. Otlyotov − *N.N. Semenov Federal Research Center for Chemical Physics RAS, 119991 Moscow, Russian Federation;* orcid.org/0000-0001-6974-6327

Complete contact information is available at: https://pubs.acs.org/10.1021/acs.inorgchem.5c03069

Author Contributions

The manuscript was written through contributions of all authors. All authors have given approval to the final version of the manuscript.

Funding

This work was financially supported by the Russian Science Foundation (project 24−23−00302).

Notes

The authors declare no competing financial interest.

ACKNOWLEDGMENTS

This work was financially supported by the Russian Science Foundation (project 24-23-00302).

REFERENCES

(1) Lübken, D.; Saxarra, M.; Kalesse, M. Tris(Acetylacetonato) Iron(III): Recent Developments and Synthetic Applications. *Synthesis* **2019**, *51* (1), 161−177.

(2) Qian, W.; Chen, Z.; Cottingham, S.; Merrill, W. A.; Swartz, N. A.; Goforth, A. M.; Clare, T. L.; Jiao, J. Surfactant-Free Hybridization of Transition Metal Oxide Nanoparticles with Conductive Graphene for High-Performance Supercapacitor. *Green Chem.* **2012**, *14* (2), 371−377.

(3) Zhang, Z.; Wong, C. P. Study on the Catalytic Behavior of Metal Acetylacetonates for Epoxy Curing Reactions. *J. Appl. Polym. Sci.* **2002**, *86* (7), 1572−1579.

(4) Sodhi, R. K.; Paul, S. An Overview of Metal Acetylacetonates: Developing Areas/Routes to New Materials and Applications in Organic Syntheses. *Catal. Surv. Asia* **2018**, *22*, 31−62.

(5) Munawar, A.; Durrani, A.; Durrani, A. K. Study of Transition Metal Acetylacetonate Doped PVC Films Introduction. *J. Fac. Eng. Technol.* **2015**, *22* (1), 317−328.

(6) Zherikova, K. V.; Zelenina, L. N.; Chusova, T. P.; Morozova, N. B.; Trubin, S. V.; Vikulova, E. S. Scandium(III) Beta-Diketonate Derivatives as Precursors for Oxide Film Deposition by CVD. *Phys. Procedia* **2013**, *46*, 200−208.

(7) Fleeting, K. A.; Davies, H. O.; Jones, A. C.; O'Brien, P.; Leedham, T. J.; Crosbie, M. J.; Wright, P. J.; Williams, D. J. Developing the Chemistry of Novel Scandium β-Diketonates for the MOCVD of Scandium-Containing Oxides. *Chem. Vap. Deposition* **1999**, *5* (6), 261−264.

(8) Makarenko, A. M.; Zaitsau, D. H.; Zherikova, K. V. Metal-Organic Chemical Vapor Deposition Precursors: Diagnostic Check for Volatilization Thermodynamics of Scandium(III) β-Diketonates. *Coatings* **2023**, *13* (3), No. 535.

(9) Sodhi, R. K.; Paul, S. An Overview of Metal Acetylacetonates: Developing Areas/Routes to New Materials and Applications in Organic Syntheses. *Catal. Surv. Asia* **2018**, *22*, 31−62, DOI: 10.1007/s10563-017-9239-9.

(10) Weng, S. S.; Ke, C. S.; Chen, F. K.; Lyu, Y. F.; Lin, G. Y. Transesterification Catalyzed by Iron(III) β-Diketonate Species. *Tetrahedron* **2011**, *67* (9), 1640−1648.

(11) Umare, P. S.; Tembe, G. L. Catalytic Oxidative Coupling of 2-Naphthol Using Metal β-Diketonates. In *Reaction Kinetics and Catalysis Letters*; Kluwer Academic Publishers, 2004; Vol. *82*, pp 173−178.

(12) Struzinski, T. H.; Von Gohren, L. R.; Roy MacArthur, A. H. Modified Cobalt(II) Acetylacetonate Complexes as Catalysts for Negishi-Type Coupling Reactions: Influence of Ligand Electronic Properties on Catalyst Activity. *Transition Met. Chem.* **2009**, *34* (6), 637−640.

(13) Ma, Y.; Reardon, D.; Gambarotta, S.; Yap, G.; Zahalka, H.; Lemay, C. Vanadium-Catalyzed Ethylene-Propylene Copolymerization: The Question of the Metal Oxidation State in Ziegler-Natta Polymerization Promoted by (β-Diketonate)3V. *Organometallics* **1999**, *18* (15), 2773−2781.

(14) Ban, H. T.; Kase, T.; Murata, M. Manganese-Based Transition Metal Complexes as New Catalysts for Olefin Polymerizations. *J. Polym. Sci., Part A:Polym. Chem.* **2001**, *39* (21), 3733−3738.

(15) Liu, Q.; Shinkle, A. A.; Li, Y.; Monroe, C. W.; Thompson, L. T.; Sleightholme, A. E. S. Non-Aqueous Chromium Acetylacetonate Electrolyte for Redox Flow Batteries. *Electrochem. Commun.* **2010**, *12* (11), 1634−1637.

(16) Liu, Q.; Sleightholme, A. E. S.; Shinkle, A. A.; Li, Y.; Thompson, L. T. Non-Aqueous Vanadium Acetylacetonate Electrolyte for Redox Flow Batteries. *Electrochem. Commun.* **2009**, *11* (12), 2312−2315.

(17) Otlyotov, A. A.; Minenkov, Y.; Zaitsau, D. H.; Zherikova, K. V.; Verevkin, S. P. "In Vitro" and "In Vivo" Diagnostic Check for the Thermochemistry of Metal−Organic Compounds. *Inorg. Chem.* **2022**, *61* (28), 10743−10755.

(18) Makarenko, A. M.; Trubin, S. V.; Zherikova, K. V. Breaking through the Thermodynamics "Wilds" of Metal−Organic Chemical Vapor Deposition Precursors: Metal Tris-Acetylacetonates. *Coatings* **2023**, *13* (8), No. 1458.

(19) Raghavachari, K.; Saha, A. Accurate Composite and Fragment-Based Quantum Chemical Models for Large Molecules. *Chem. Rev.* **2015**, *115* (12), 5643−5677.

(20) Karton, A. A Computational Chemist's Guide to Accurate Thermochemistry for Organic Molecules. *WIREs Comput. Mol. Sci.* **2016**, *6* (3), 292−310.

(21) Raghavachari, K.; Trucks, G. W.; Pople, J. A.; Head-Gordon, M. A Fifth-Order Perturbation Comparison of Electron Correlation Theories. *Chem. Phys. Lett.* **1989**, *157* (6), 479−483.

(22) Neese, F.; Hansen, A.; Liakos, D. G. Efficient and Accurate Approximations to the Local Coupled Cluster Singles Doubles Method Using a Truncated Pair Natural Orbital Basis. *J. Chem. Phys.* **2009**, *131* (6), No. 064103.
(23) Neese, F.; Wennmohs, F.; Hansen, A. Efficient and Accurate Local Approximations to Coupled-Electron Pair Approaches: An Attempt to Revive the Pair Natural Orbital Method. *J. Chem. Phys.* **2009**, *130* (11), No. 114108.
(24) Riplinger, C.; Neese, F. An Efficient and near Linear Scaling Pair Natural Orbital Based Local Coupled Cluster Method. *J. Chem. Phys.* **2013**, *138* (3), No. 034106.
(25) Riplinger, C.; Sandhoefer, B.; Hansen, A.; Neese, F. Natural Triple Excitations in Local Coupled Cluster Calculations with Pair Natural Orbitals. *J. Chem. Phys.* **2013**, *139* (13), No. 134101.
(26) Riplinger, C.; Pinski, P.; Becker, U.; Valeev, E. F.; Neese, F. Sparse Maps—A Systematic Infrastructure for Reduced-Scaling Electronic Structure Methods. II. Linear Scaling Domain Based Pair Natural Orbital Coupled Cluster Theory. *J. Chem. Phys.* **2016**, *144* (2), No. 024109.
(27) Bistoni, G.; Riplinger, C.; Minenkov, Y.; Cavallo, L.; Auer, A. A.; Neese, F. Treating Subvalence Correlation Effects in Domain Based Pair Natural Orbital Coupled Cluster Calculations: An Out-of-the-Box Approach. *J. Chem. Theory Comput* **2017**, *13* (7), 3220−3227.
(28) Saitow, M.; Becker, U.; Riplinger, C.; Valeev, E. F.; Neese, F. A New Near-Linear Scaling, Efficient and Accurate, Open-Shell Domain-Based Local Pair Natural Orbital Coupled Cluster Singles and Doubles Theory. *J. Chem. Phys.* **2017**, *146* (16), No. 164105.
(29) Feller, D.; Peterson, K. A.; Dixon, D. A. The Impact of Larger Basis Sets and Explicitly Correlated Coupled Cluster Theory on the Feller−Peterson−Dixon Composite Method. *Annu. Rep. Comput. Chem.* **2016**, *12*, 47−78.
(30) Dixon, D. A.; Feller, D.; Peterson, K. A. A Practical Guide to Reliable First Principles Computational Thermochemistry Predictions across the Periodic Table. In *Annual Reports in Computational Chemistry*; Ralph, A. W., Ed.; Elsevier: Amsterdam, 2012; pp 1−28.
(31) Feller, D.; Peterson, K. A.; Dixon, D. A. Further Benchmarks of a Composite, Convergent, Statistically Calibrated Coupled-Cluster-Based Approach for Thermochemical and Spectroscopic Studies. *Mol. Phys.* **2012**, *110* (19−20), 2381−2399.
(32) Minenkova, I.; Otlyotov, A. A.; Cavallo, L.; Minenkov, Y. Gas-Phase Thermochemistry of Polycyclic Aromatic Hydrocarbons: An Approach Integrating the Quantum Chemistry Composite Scheme and Reaction Generator. *Phys. Chem. Chem. Phys.* **2022**, *24* (5), 3163−3181.
(33) Nosach, E. A.; Rozov, T. P.; Otlyotov, A. A.; Minenkov, Y. Efficient Reaction-Based Approaches for Gas-Phase Enthalpy of Formation Prediction and Their Application to Large (C32) Polycyclic Aromatic Hydrocarbons. *Adv. Theory Simul.* **2024**, *7*, No. 2400319.
(34) Otlyotov, A. A.; Kurochkin, I. Y.; Minenkov, Y.; Trapp, P. C.; Lamm, J. H.; Girichev, G. V.; Mitzel, N. W. Gas-Phase Equilibrium Molecular Structures and Ab Initio Thermochemistry of Anthracene and Rubrene. *Phys. Chem. Chem. Phys.* **2022**, *24* (47), 29195−29204.
(35) Otlyotov, A. A.; Moshchenkov, A. D.; Minenkov, Y. Ni, Cu, Zn, Pd, Ag and Cd Tetraphenylporphyrin Ab Initio Thermochemistry: Enthalpy of Formation of ZnTPP Revisited. *Inorg. Chem.* **2024**, *63*, 10230−10239.
(36) Chaikin, A. V.; Rozov, T. P.; Ryzhako, A. S.; Moshchenkov, A. D.; Otlyotov, A. A.; Minenkov, Y. The Simpler the Better? Enthalpies of Formation and Entropies of Short-Chain Chlorinated Paraffins by Ab Initio, DFT, Group Additivity and Semiempirical Approximations. *J. Mol. Graphics Modell.* **2025**, *140*, No. 109106.
(37) Rozov, T. P.; Chaikin, A. V.; Moshchenkov, A. D.; Ryzhako, A. S.; Otlyotov, A. A.; Minenkov, Y. Accurate Gas-Phase Thermochemistry of Commercially Utilized Brominated Flame Retardants. *Chem. Phys. Lett.* **2025**, *878*, No. 142256.
(38) Ruscic, B.; Bross, D. H. Accurate and Reliable Thermochemistry by Data Analysis of Complex Thermochemical Networks Using Active Thermochemical Tables: The Case of Glycine Thermochemistry. *Faraday Discuss.* **2025**, *256* (0), 345−372.
(39) Ruscic, B.; Pinzon, R. E.; Von Laszewski, G.; Kodeboyina, D.; Burcat, A.; Leahy, D.; Montoy, D.; Wagner, A. F. Active Thermochemical Tables: Thermochemistry for the 21st Century. *J. Phys. Conf. Ser.* **2005**, *16* (1), 561−570.
(40) Ruscic, B.; Pinzon, R. E.; Morton, M. L.; von Laszevski, G.; Bittner, S. J.; Nijsure, S. G.; Amin, K. A.; Minkoff, M.; Wagner, A. F. Introduction to Active Thermochemical Tables: Several "Key" Enthalpies of Formation Revisited. *J. Phys. Chem. A* **2004**, *108* (45), 9979−9997.
(41) Ruscic, B.; Bross, D. H. *Active Thermochemical Tables (ATcT) Values Based on Ver. 1.202 of the Thermochemical Network*, Argonne National Laboratory, 2024; Available at: ATcT.Anl.Gov.
(42) Adamo, C.; Barone, V. Toward Reliable Density Functional Methods without Adjustable Parameters: The PBE0 Model. *J. Chem. Phys.* **1999**, *110* (13), 6158−6170.
(43) Weigend, F.; Ahlrichs, R. Balanced Basis Sets of Split Valence, Triple Zeta Valence and Quadruple Zeta Valence Quality for H to Rn: Design and Assessment of Accuracy. *Phys. Chem. Chem. Phys.* **2005**, *7* (18), 3297−3305.
(44) Neese, F. Software Update: The ORCA Program System—Version 5.0. *WIREs Comput. Mol. Sci.* **2022**, *12*, No. e1606, DOI: 10.1002/wcms.1606.
(45) Grimme, S.; Ehrlich, S.; Goerigk, L. Effect of the Damping Function in Dispersion Corrected Density Functional Theory. *J. Comput. Chem.* **2011**, *32* (7), 1456−1465.
(46) Grimme, S.; Antony, J.; Ehrlich, S.; Krieg, H. A Consistent and Accurate Ab Initio Parametrization of Density Functional Dispersion Correction (DFT-D) for the 94 Elements H-Pu. *J. Chem. Phys.* **2010**, *132* (15), No. 154104.
(47) Neese, F.; Wennmohs, F.; Hansen, A.; Becker, U. Efficient, Approximate and Parallel Hartree-Fock and Hybrid DFT Calculations. A "chain-of-Spheres" Algorithm for the Hartree-Fock Exchange. *Chem. Phys.* **2009**, *356* (1−3), 98−109.
(48) Neese, F. An Improvement of the Resolution of the Identity Approximation for the Formation of the Coulomb Matrix. *J. Comput. Chem.* **2003**, *24* (14), 1740−1747.
(49) Weigend, F. Accurate Coulomb-Fitting Basis Sets for H to Rn. *Phys. Chem. Chem. Phys.* **2006**, *8* (9), 1057−1065.
(50) Bakowies, D.; Von Lilienfeld, O. A. Density Functional Geometries and Zero-Point Energies in Ab Initio Thermochemical Treatments of Compounds with First-Row Atoms (H, C, N, O, F). *J. Chem. Theory Comput.* **2021**, *17* (8), 4872−4890.
(51) Pracht, P.; Grimme, S. Calculation of Absolute Molecular Entropies and Heat Capacities Made Simple. *Chem. Sci.* **2021**, *12* (19), 6551−6568.
(52) Grimme, S. Supramolecular Binding Thermodynamics by Dispersion-Corrected Density Functional Theory. *Chem. - Eur. J.* **2012**, *18* (32), 9955−9964.
(53) Otlyotov, A. A.; Minenkov, Y. Gas-Phase Thermochemistry of Noncovalent Ligand−Alkali Metal Ion Clusters: An Impact of Low Frequencies. *J. Comput. Chem.* **2023**, *44* (22), 1807−1816.
(54) Tverdova, N. V.; Girichev, G. V.; Shlykov, S. A.; Kuz'mina, N. P.; Petrova, A. A.; Zaitseva, I. G. A Study of the Structure and Energy of β-Diketonates. XVIII. Molecular Structure of Chromium and Cobalt Tris-Acetylacetonates According to Quantum Chemical Calculations and Gas Electron Diffraction. *J. Struct. Chem.* **2013**, *54* (5), 863−875.
(55) Berger, R. J. F.; Girichev, G.; Petrova, A.; Sliznev, V.; Tverdova, N.; Giricheva, N. Molecular Structure of Manganese Tris-Acetylacetonate in Different Spin States. *Izv. Vyssh. Uchebn. Zaved. Khim. Khim. Tekhnol.* **2017**, *60* (4), 47−53.
(56) Berger, R. J. F.; Girichev, G. V.; Giricheva, N. I.; Petrova, A. A.; Tverdova, N. V. The Structure of $Mn(Acac)_3$—Experimental Evidence of a Static Jahn−Teller Effect in the Gas Phase. *Angew. Chem., Int. Ed.* **2017**, *56* (49), 15751−15754.
(57) Petrova, A. A.; Tverdova, N. V.; Giricheva, N. I.; Girichev, G. V. Molecular Structure of Tris(Acetylacetonate)Iron Studied by

Gasphase Electron Diffraction and DFT Calculations. *Izv. Vyssh. Uchebn. Zaved. Khim. Khim. Tekhnol.* **2017**, *60* (3), 97−99.
(58) Girichev, G. V.; Tverdova, N. V.; Giricheva, N. I.; Shlykov, S. A. The Molecular Species in Saturated and Overheated Vapors of $Sc(Acac)_3$: A First Structural Study of Bis-Acetylacetonate Scandium $Sc(Acac)_2$ Radical. *Chem. Phys. Lett.* **2022**, *806*, No. 139989.
(59) Diaz-Acosta, I.; Baker, J.; Cordes, W.; Pulay, P. Calculated and Experimental Geometries and Infrared Spectra of Metal Tris-Acetylacetonates: Vibrational Spectroscopy as a Probe of Molecular Structure for Ionic Complexes. Part I. *J. Phys. Chem. A* **2001**, *105* (1), 238−244.
(60) Diaz-Acosta, I.; Baker, J.; Hinton, J. F.; Pulay, P. Calculated and Experimental Geometries and Infrared Spectra of Metal Tris-Acetylacetonates: Vibrational Spectroscopy as a Probe of Molecular Structure for Ionic Complexes. Part II. *Spectrochim. Acta, Part A* **2003**, *59* (2), 363−377.
(61) Dunning, T. H. Gaussian Basis Sets for Use in Correlated Molecular Calculations. I. The Atoms Boron through Neon and Hydrogen. *J. Chem. Phys.* **1989**, *90* (2), 1007−1023.
(62) Woon, D. E.; Dunning, T. H. Gaussian-Basis Sets for Use in Correlated Molecular Calculations. III. The Atoms Aluminum through Argon. *J. Chem. Phys.* **1993**, *98* (2), 1358−1371.
(63) Peterson, K. A. Private Communication. 2019.
(64) Dolg, M. Improved Relativistic Energy-Consistent Pseudopotentials for 3d-Transition Metals. *Theor. Chem. Acc.* **2005**, *114* (4), 297−304.
(65) Minenkov, Y.; Cavallo, L.; Peterson, K. A. Influence of the Complete Basis Set Approximation, Tight Weighted-Core, and Diffuse Functions on the DLPNO-CCSD(T1) Atomization Energies of Neutral H,C,O-Compounds. *J. Comput. Chem.* **2023**, *44* (5), 687−696.
(66) Feller, D.; Peterson, K. A.; Grant Hill, J. On the Effectiveness of CCSD(T) Complete Basis Set Extrapolations for Atomization Energies. *J. Chem. Phys.* **2011**, *135* (4), No. 044102.
(67) Martin, J. M. L. Ab Initio Total Atomization Energies of Small Molecules — towards the Basis Set Limit. *Chem. Phys. Lett.* **1996**, *259* (5−6), 669−678.
(68) Weigend, F.; Kohn, A.; Hättig, C. Efficient Use of the Correlation Consistent Basis Sets in Resolution of the Identity MP2 Calculations. *J. Chem. Phys.* **2002**, *116* (8), 3175−3183.
(69) Stoychev, G. L.; Auer, A. A.; Neese, F. Automatic Generation of Auxiliary Basis Sets. *J. Chem. Theory Comput.* **2017**, *13* (2), 554−562.
(70) Altun, A.; Neese, F.; Bistoni, G. Extrapolation to the Limit of a Complete Pair Natural Orbital Space in Local Coupled-Cluster Calculations. *J. Chem. Theory Comput.* **2020**, *16* (10), 6142−6149.
(71) Guo, Y.; Riplinger, C.; Becker, U.; Liakos, D. G.; Minenkov, Y.; Cavallo, L.; Neese, F. Communication: An Improved Linear Scaling Perturbative Triples Correction for the Domain Based Local Pair-Natural Orbital Based Singles and Doubles Coupled Cluster Method [DLPNO-CCSD(T)]. *J. Chem. Phys.* **2018**, *148* (1), No. 011101.
(72) Guo, Y.; Riplinger, C.; Liakos, D. G.; Becker, U.; Saitow, M.; Neese, F. Linear Scaling Perturbative Triples Correction Approximations for Open-Shell Domain-Based Local Pair Natural Orbital Coupled Cluster Singles and Doubles Theory [DLPNO-CCSD(T/T)]. *J. Chem. Phys.* **2020**, *152* (2), No. 024116.
(73) Balabanov, N. B.; Peterson, K. A. Systematically Convergent Basis Sets for Transition Metals. I. All-Electron Correlation Consistent Basis Sets for the 3d Elements Sc-Zn. *J. Chem. Phys.* **2005**, *123* (6), No. 064107.
(74) De Jong, W. A.; Harrison, R. J.; Dixon, D. A. Parallel Douglas-Kroll Energy and Gradients in NWChem: Estimating Scalar Relativistic Effects Using Douglas-Kroll Contracted Basis Sets. *J. Chem. Phys.* **2001**, *114* (1), 48−53.
(75) Dunning, T. H. Gaussian-Basis Sets for Use in Correlated Molecular Calculations. 1. The Atoms Boron through Neon and Hydrogen. *J. Chem. Phys.* **1989**, *90* (2), 1007−1023.
(76) Woon, D. E.; Dunning, T. H. Gaussian Basis Sets for Use in Correlated Molecular Calculations. III. The Atoms Aluminum through Argon. *J. Chem. Phys.* **1993**, *98* (2), 1358−1371.
(77) *Thermochemistry Program*, https://Github.Com/QuantumChemistryGroup/Thermochemistry. (Accessed March 12, 2025).
(78) Ercolani, G. Numerical Evaluation of Energy Levels and Wave Functions for Hindered Internal Rotation. *J. Chem. Educ.* **2000**, *77* (11), 1495.
(79) Minenkov, Y.; Occhipinti, G.; Heyndrickx, W.; Jensen, V. R. The Nature of the Barrier to Phosphane Dissociation from Grubbs Olefin Metathesis Catalysts. *Eur. J. Inorg. Chem.* **2012**, *2012*, 1507−1516.
(80) Ryzhako, A. S.; Tuma, A. A.; Otlyotov, A. A.; Minenkov, Y. An Influence of Electronic Structure Theory Method, Thermodynamic and Implicit Solvation Corrections on the Organic Carbonates Conformational and Binding Energies. *J. Comput. Chem.* **2024**, *45* (32), 3004−3016.
(81) Dohm, S.; Hansen, A.; Steinmetz, M.; Grimme, S.; Checinski, M. P. Comprehensive Thermochemical Benchmark Set of Realistic Closed-Shell Metal Organic Reactions. *J. Chem. Theory Comput.* **2018**, *14* (5), 2596−2608.
(82) Maurer, L. R.; Bursch, M.; Grimme, S.; Hansen, A. Assessing Density Functional Theory for Chemically Relevant Open-Shell Transition Metal Reactions. *J. Chem. Theory Comput.* **2021**, *17* (10), 6134−6151.
(83) Bursch, M.; Mewes, J.; Hansen, A.; Grimme, S. Best-Practice DFT Protocols for Basic Molecular Computational Chemistry. *Angew. Chem., Int. Ed.* **2022**, *61* (42), No. e202205735.
(84) Mardirossian, N.; Head-Gordon, M. ωB97M-V: A Combinatorially Optimized, Range-Separated Hybrid, Meta-GGA Density Functional with VV10 Nonlocal Correlation. *J. Chem. Phys.* **2016**, *144* (21), No. 214110.
(85) Grimme, S. Semiempirical Hybrid Density Functional with Perturbative Second-Order Correlation. *J. Chem. Phys.* **2006**, *124* (3), No. 034108.
(86) Caldeweyher, E.; Bannwarth, C.; Grimme, S. Extension of the D3 Dispersion Coefficient Model. *J. Chem. Phys.* **2017**, *147* (3), No. 034112.
(87) Caldeweyher, E.; Ehlert, S.; Hansen, A.; Neugebauer, H.; Spicher, S.; Bannwarth, C.; Grimme, S. A Generally Applicable Atomic-Charge Dependent London Dispersion Correction. *J. Chem. Phys.* **2019**, *150* (15), No. 154122.
(88) Caldeweyher, E.; Mewes, J. M.; Ehlert, S.; Grimme, S. Extension and Evaluation of the D4 London-Dispersion Model for Periodic Systems. *Phys. Chem. Chem. Phys.* **2020**, *22* (16), 8499−8512.
(89) Zhao, Y.; Truhlar, D. G. The M06 Suite of Density Functionals for Main Group Thermochemistry, Thermochemical Kinetics, Noncovalent Interactions, Excited States, and Transition Elements: Two New Functionals and Systematic Testing of Four M06-Class Functionals and 12 Other Functionals. *Theor. Chem. Acc.* **2008**, *120* (1−3), 215−241.
(90) Weigend, F.; Ahlrichs, R. Balanced Basis Sets of Split Valence, Triple Zeta Valence and Quadruple Zeta Valence Quality for H to Rn: Design and Assessment of Accuracy. *Phys. Chem. Chem. Phys.* **2005**, *7* (18), 3297−3305.
(91) Vydrov, O. A.; Van Voorhis, T. Nonlocal van Der Waals Density Functional: The Simpler the Better. *J. Chem. Phys.* **2010**, *133* (24), No. 244103.
(92) Lehtola, S.; Steigemann, C.; Oliveira, M. J. T.; Marques, M. A. L. Recent Developments in LIBXC — A Comprehensive Library of Functionals for Density Functional Theory. *SoftwareX* **2018**, *7*, 1−5.
(93) Kossmann, S.; Neese, F. Efficient Structure Optimization with Second-Order Many-Body Perturbation Theory: The RIJCOSX-MP2 Method. *J. Chem. Theory Comput* **2010**, *6* (8), 2325−2338.
(94) Helmich-Paris, B.; de Souza, B.; Neese, F.; Izsák, R. An Improved Chain of Spheres for Exchange Algorithm. *J. Chem. Phys.* **2021**, *155* (10), No. 104109.
(95) Ruscic, B.; Bross, D. H.Thermochemistry. In *Computer Aided Chemical Engineering*; Elsevier, 2019; Vol. *45*, pp 3−114 .

https://doi.org/10.1021/acs.inorgchem.5c03069
Inorg. Chem. 2025, 64, 21405−21418

(96) Ruscic, B. Uncertainty Quantification in Thermochemistry, Benchmarking Electronic Structure Computations, and Active Thermochemical Tables. *Int. J. Quantum Chem.* **2014**, *114* (17), 1097−1101.
(97) Moshchenkov, A. D.; Otlyotov, A. A.; Minenkov, Y. Accurate Ab Initio Thermochemistry of the Groups 10−12 Difluorides, Dichlorides, Oxides and Sulfides. *J. Chem. Thermodyn.* **2023**, *187*, No. 107151.
(98) DeYonker, N. J.; Peterson, K. A.; Steyl, G.; Wilson, A. K.; Cundari, T. R. Quantitative Computational Thermochemistry of Transition Metal Species. *J. Phys. Chem. A* **2007**, *111* (44), 11269−11277.
(99) Belova, N. V.; Oberhammer, H.; Trang, N. H.; Girichev, G. V. Tautomeric Properties and Gas-Phase Structure of Acetylacetone. *J. Org. Chem.* **2014**, *79* (12), 5412−5419.
(100) Iorish, V. S.; Yungman, V. S. *Online Database "Thermal Constants of Compounds."*.
(101) Osina, E. L.; Gorokhov, L. N. New Value of the Enthalpy of Formation of ScF_3 Molecules. *High Temp.* **2017**, *55* (4), 615−617.
(102) Hildenbrand, D. L.; Lau, K. H. Thermochemical Properties of the Gaseous Scandium, Yttrium, and Lanthanum Fluorides. *J. Chem. Phys.* **1995**, *102* (9), 3769−3775.
(103) Osina, E. L.; Osin, S. B. Thermodynamics of the Evaporation of Scandium Trifluoride and the Composition of Its Vapor. *High Temp.* **2022**, *60* (1), 41−44.
(104) Osina, E. L.; Gusarov, A. V. Thermodynamic Functions and Formation Enthalpies of Scandium Trihalides Molecules. *High Temp.* **2015**, *53* (6), 817−822.
(105) Zmbov, K. F.; Margrave, J. L. Mass Spectrometry at High Temperatures. XVIII. The Stabilities of the Mono- and Difluorides of Scandium and Yttrium. *J. Chem. Phys.* **1967**, *47* (9), 3122−3125.
(106) Minenkova, I.; Osina, E. L.; Cavallo, L.; Minenkov, Y. Gas-Phase Thermochemistry of MX_3 and M_2X_6 (M = Sc, Y; X = F, Cl, Br, I) from a Composite Reaction-Based Approach: Homolytic versus Heterolytic Cleavage. *Inorg. Chem.* **2020**, *59* (23), 17084−17095.
(107) Solomonik, V. G.; Mukhanov, A. A. Ab Initio Study of Scandium Fluoride Molecules: ScF, ScF_2, and ScF_3. *J. Struct. Chem.* **2012**, *53* (1), 28−34.
(108) Jiang, W.; Deyonker, N. J.; Determan, J. J.; Wilson, A. K. Toward Accurate Theoretical Thermochemistry of First Row Transition Metal Complexes. *J. Phys. Chem. A* **2012**, *116* (2), 870−885.
(109) Mayhall, N. J.; Raghavachari, K.; Redfern, P. C.; Curtiss, L. A. Investigation of Gaussian4 Theory for Transition Metal Thermochemistry. *J. Phys. Chem. A* **2009**, *113* (17), 5170−5175.
(110) Gole, J. L.; Chalek, C. L.; Mason, M. M.; De Melo, G. F.; Vasiliu, M.; Dixon, D. A. Observation of Selectively Populated Monohalide Excited States from the Reactions of Group 3 Metal (Sc, Y, and La) Monomers and Dimers with Halogen-Containing Molecules. *J. Phys. Chem. A* **2022**, *126* (22), 3403−3426.
(111) Chase, M. *NIST-JANAF Thermochemical Tables*, 4th ed.; American Institute of Physics, 1998.
(112) Pan, Y.; Luo, Z.; Chang, Y. C.; Lau, K. C.; Ng, C. Y. High-Level Ab Initio Predictions for the Ionization Energies, Bond Dissociation Energies, and Heats of Formation of Titanium Oxides and Their Cations (TiO_n/TiO_n^+, n = 1 and 2). *J. Phys. Chem. A* **2017**, *121* (3), 669−679.
(113) Li, S.; Hennigan, J. M.; Dixon, D. A.; Peterson, K. A. Accurate Thermochemistry for Transition Metal Oxide Clusters. *J. Phys. Chem. A* **2009**, *113* (27), 7861−7877.
(114) Wang, T. H.; Navarrete-López, A. M.; Li, S.; Dixon, D. A.; Gole, J. L. Hydrolysis of $TiCl_4$: Initial Steps in the Production of TiO 2. *J. Phys. Chem. A* **2010**, *114* (28), 7561−7570.
(115) Fang, Z.; Lee, Z.; Peterson, K. A.; Dixon, D. A. Use of Improved Orbitals for CCSD(T) Calculations for Predicting Heats of Formation of Group IV and Group VI Metal Oxide Monomers and Dimers and UCl_6. *J. Chem. Theory Comput.* **2016**, *12* (8), 3583−3592.
(116) Li, S.; Dixon, D. A. Molecular Structures and Energetics of the $(TiO_2)_n$ (n = 1−4) Clusters and Their Anions. *J. Phys. Chem. A* **2008**, *112* (29), 6646−6666.
(117) Minenkov, Y.; Sliznev, V. V.; Cavallo, L. Accurate Gas Phase Formation Enthalpies of Alloys and Refractories Decomposition Products. *Inorg. Chem.* **2017**, *56* (3), 1386−1401.
(118) Thanthiriwatte, K. S.; Vasiliu, M.; Battey, S. R.; Lu, Q.; Peterson, K. A.; Andrews, L.; Dixon, D. A. Gas Phase Properties of MX_2 and MX_4 (X = F, Cl) for M = Group 4, Group 14, Cerium, and Thorium. *J. Phys. Chem. A* **2015**, *119* (22), 5790−5803.
(119) Cox, J. D.; Wagman, D. D.; Medvedev, V. A. *CODATA Key Values for Thermodynamics*; Hemisphere Publishing Corp.: New York, 1989.
(120) Farber, M.; Darnell, A. J. Heat of Formation and Entropy of Titanium Tetrachloride from an Investigation of the Equilibrium: $TiO_{2(s)}+4HCl_{(g)} = TiCl_{4(g)}+2H_3O_{(g)}$. *J. Chem. Phys.* **1955**, *23* (8), 1460−1463.
(121) *CRC Handbook of Chemistry and Physics*, Internet version 2005; Lide, D. R., Ed.; CRC Press: Boca Raton, FL, 2005.
(122) Koukkari, P.; Paiva, E. Mechanistic and Constrained Thermochemical Modelling in Chemical Reactor Engineering: Ti(IV) Chloride Oxidation Revisited. *Chem. Eng. Sci.* **2018**, *179*, 227−242.
(123) West, R. H.; Beran, G. J. O.; Green, W. H.; Kraft, M. First-Principles Thermochemistry for the Production of TiO_2 from $TiCl_4$. *J. Phys. Chem. A* **2007**, *111* (18), 3560−3565.
(124) Ge, Y.; Deprekel, D.; Lam, K. T.; Ngo, K.; Vo, P. Assessing Density Functionals for the Prediction of Thermochemistry of Ti-O-Cl Species. *J. Theor Comput. Chem.* **2015**, *14* (8), No. 1550055.
(125) Balducci, G.; Gigli, G.; Guido, M. Thermochemical Properties of the Gaseous Molecules VO, VO_2, and V_2O_4. *J. Chem. Phys.* **1983**, *79* (11), 5616−5622.
(126) Fang, Z.; Vasiliu, M.; Peterson, K. A.; Dixon, D. A. Prediction of Bond Dissociation Energies/Heats of Formation for Diatomic Transition Metal Compounds: CCSD(T) Works. *J. Chem. Theory Comput* **2017**, *13* (3), 1057−1066.
(127) Bross, D. H.; Hill, J. G.; Werner, H. J.; Peterson, K. A. Explicitly Correlated Composite Thermochemistry of Transition Metal Species. *J. Chem. Phys.* **2013**, *139* (9), No. 094302.
(128) Deyonker, N. J.; Williams, T. G.; Imel, A. E.; Cundari, T. R.; Wilson, A. K. Accurate Thermochemistry for Transition Metal Complexes from First-Principles Calculations. *J. Chem. Phys.* **2009**, *131* (2), No. 024106.
(129) Ebbinghaus, B. B. Thermodynamics of Gas Phase Chromium Species: The Chromium Oxides, the Chromium Oxyhydroxides, and Volatility Calculations in Waste Incineration Processes. *Combust. Flame* **1993**, *93*, 119−137.
(130) Welch, B. K.; Wilson, A. K. Super-Correlation Consistent Composite Approach (s-CcCA) for the Late 3d and 4d Transition Metals: Impact of Higher-Order Excitations on Thermochemical Prediction. *Chem. Phys. Lett.* **2024**, *849*, No. 141423.
(131) Chan, B.; Karton, A.; Raghavachari, K.; Radom, L. Heats of Formation for CrO, CrO_2, and CrO_3: An Extreme Challenge for Black-Box Composite Procedures. *J. Chem. Theory Comput* **2012**, *8* (9), 3159−3166.
(132) Li, S.; Guenther, C. L.; Kelley, M. S.; Dixon, D. A. Molecular Structures, Acid-Base Properties, and Formation of Group 6 Transition Metal Hydroxides. *J. Phys. Chem. C* **2011**, *115* (16), 8072−8103.
(133) Hildenbrand, D. L. Dissociation Energies of the Monochlorides and Dichlorides of Cr, Mn, Fe, Co, and Ni. *J. Chem. Phys.* **1995**, *103* (7), 2634−2641.
(134) Hildenbrand, D. L. Low-Lying Electronic States and Dissociation Energies of the Monochlorides of Cr, Mn, Fe, Co, and Ni. *J. Phys. Chem. A* **2008**, *112* (17), 3813−3815.
(135) Nielsen, I. M. B.; Allendorf, M. D. High-Level Ab Initio Thermochemical Data for Halides of Chromium, Manganese, and Iron. *J. Phys. Chem. A* **2005**, *109* (5), 928−933.
(136) Kent, R. A.; Ehlert, T. C.; Margrave, J. L. Mass Spectrometric Studies at High Temperatures. V. The Sublimation Pressure of

https://doi.org/10.1021/acs.inorgchem.5c03069
Inorg. Chem. 2025, 64, 21405−21418

Manganese. *Journal of American Chemical Society* **1984**, *86* (23), 5090−5093.
(137) Ehlert, T. C.; Hsia, M. Mass Spectrometric and Thermochemical Studies of the Manganese Fluorides. *J. Fluorine Chem.* **1972**, *2* (1), 33−51.
(138) Balducci, G.; Campodonico, M.; Gigli, G.; Meloni, G.; Nunziante Cesaro, S. Experimental and Computational Study of the New Gaseous Molecules OMnF and $OMnF_2$. *J. Chem. Phys.* **2002**, *117* (23), 10613−10620.
(139) Bach, R. D.; Shobe, D. S.; Schlegel, H. B.; Nagel, C. J. Thermochemistry of Iron Chlorides and Their Positive and Negative Ions. *J. Phys. Chem. A* **1996**, *100* (21), 8770−8776.
(140) Xu, X.; Zhang, W.; Tang, M.; Truhlar, D. G. Do Practical Standard Coupled Cluster Calculations Agree Better than Kohn−Sham Calculations with Currently Available Functionals When Compared to the Best Available Experimental Data for Dissociation Energies of Bonds to 3d Transition Metals? *J. Chem. Theory Comput* **2015**, *11* (5), 2036−2052.
(141) Wood, J. L.; Jones, M. M. Coordinate Bond Energies and Inner Orbital Splitting in Some Tervalent Transition Metal Acetylacetonates. *Inorg. Chem.* **1964**, *3* (11), 1553−1556.
(142) da Silva, M. A. V. R. Thermochemistry of β-Diketones and Metal-β-Diketonates. Metal-Oxygen Bond Enthalpies. In *Thermochemistry and Its Applications to Chemical and Biochemical Systems: The Thermochemistry of Molecules, Ionic Species and Free Radicals in Relation to the Understanding of Chemical and Biochemical Systems*; da Silva, M. A. V. R., Ed.; Springer Netherlands: Dordrecht, 1984; pp 317−338 DOI: 10.1007/978-94-009-6312-2_15.
(143) Jamea, E. H.; Pilcher, G. Standard Enthalpies of Formation of the Pentane-2,4-Dionate and 8-Hydroxyquinolate Complexes of Vanadium(III) and of Oxovanadium(IV) by Solution-Reaction Calorimetry. *Thermochim. Acta* **1986**, *97* (C), 77−84.
(144) Hill, J. O.; Irving, R. J. The Heat of Formation of Tris(Acetylacetonato)Manganese(III) and the Manganese-Oxygen Bond Energy. *J. Chem. Soc. A* **1968**, *0*, 3116−3118.
(145) Da Silva, M. A. V. R.; Ferrão, M. L. C. C. H.; Magalhães, A. M. L. Standard Enthalpy of Formation of Tris(2,4-Pentanedionato)-Cobalt(III): The Mean (Co-O) Bond-Dissociation Enthalpy. *Thermochim. Acta* **1988**, *129* (2), 229−235.
(146) da Silva, M. A. V. R.; Ferrao, M. L. C. C. H. Standard Enthalpies of Formation of Tris(β-Diketonate)Chromium(III) Complexes: The Mean (Cr-O) Bond-Dissociation Enthalpies. *J. Chem. Thermodyn.* **1987**, *19*, 646−652.
(147) Irving, R. J.; Hill, J. O. Standard Heat of Formation of Tris(Acetylacetonato)Chromium(III) at 25° and the Metal-Oxygen Bond Energy. *J. Chem. Soc. A* **1967**, *11*, 1413−1416.

https://doi.org/10.1021/acs.inorgchem.5c03069
Inorg. Chem. 2025, 64, 21405−21418